

University of Massachusetts Medical School

eScholarship@UMMS

GSBS Dissertations and Theses

Graduate School of Biomedical Sciences

2004-09-08

Centrosomes in Cytokinesis, Cell Cycle Progression and Ciliogenesis: a Dissertation

Agata Jurczyk

University of Massachusetts Medical School

Let us know how access to this document benefits you.

Follow this and additional works at: https://escholarship.umassmed.edu/gsbs_diss



Part of the [Amino Acids, Peptides, and Proteins Commons](#), and the [Cells Commons](#)

Repository Citation

Jurczyk A. (2004). Centrosomes in Cytokinesis, Cell Cycle Progression and Ciliogenesis: a Dissertation. GSBS Dissertations and Theses. <https://doi.org/10.13028/rt2g-d989>. Retrieved from https://escholarship.umassmed.edu/gsbs_diss/73

This material is brought to you by eScholarship@UMMS. It has been accepted for inclusion in GSBS Dissertations and Theses by an authorized administrator of eScholarship@UMMS. For more information, please contact Lisa.Palmer@umassmed.edu.

A Dissertation Presented

By

Agata Jurczyk

Submitted to the Faculty of the
University of Massachusetts Graduate School of Biomedical Sciences, Worcester

In partial fulfillment of the requirements for the degree of

DOCTOR OF PHILOSOPHY

September, 8th 2004

INTERDISCIPLINARY GRADUATE PROGRAM

COPYRIGHT NOTICE

Work presented in this dissertation has appeared in the following publications:

1. Adam Gromley, Agata Jurczyk, James Sillibourne, Ensar Halilovic, Mette Mogensen, Irina Groisman, Maureen Blomberg, and Stephen Doxsey. (2003) A novel human protein of the maternal centrioles is required for the final stages of cytokinesis and entry into S phase. *The Journal of Cell Biology*, 161 (3):535-545 (A. Gromley and A. Jurczyk contributed equally to this work).
2. Agata Jurczyk, Adam Gromley, Sambra Redick, Jovenal San Augustin, George Witman, Gregory Pazour, Dorien J.M. Peters and Stephen Doxsey. (2004) Pericentrin forms a complex with intraflagellar transport proteins and polycystin 2 and is required for primary cilia assembly. *The Journal of Cell Biology*, 166 (5):637-643.
3. Agata Jurczyk, Adam Gromley, Sambra Redick and Stephen Doxsey. Pericentrin is required for the final stages of cytokinesis and entry into S phase through its association with centriolin. In preparation for publication.

**CENTROSOMES IN CYTOKINESIS, CELL CYCLE PROGRESSION AND
CILIOGENESIS**

A Dissertation Presented

By

AGATA JURCZYK

Approved as to style and content by:

(Signature) _____
William Theurkauf, Ph.D., Chair of Committee

(Signature) _____
Craig Peterson, Ph.D., Member of Committee

(Signature) _____
Dannel McCollum, Ph.D., Member of Committee

(Signature) _____
Greenfield Sluder, Ph.D., Member of Committee

(Signature) _____
Stephen Doxsey, Ph.D., Thesis Advisor

(Signature) _____
Anthony Carruthers, Ph.D.,
Dean of the Graduate School of Biomedical Sciences

Interdisciplinary Graduate Program

September 8, 2004

ACKNOWLEDGMENTS

I would like to thank my advisor Stephen Doxsey for his mentorship, good advice and understanding of all my family emergencies. He always was flexible enough to let me juggle between home and work, what was not easy at times, but also not impossible. Special thanks to all members of Doxsey and Theurkauf Labs for all the thoughtful discussions during joined laboratory meetings and helpful suggestion on my thesis writing. Sorry, guys, but I still did not get the rationale for use of the articles. Special thanks to Sam, even though we did not work together too long, she help me a lot with many of my experiments presented in this thesis. Thanks to Adam for all of his contributions to my thesis and for all the arguments. Jim's expertise in biochemistry was instrumental to most of my presented biochemistry, he did the "impossible" (at least for me) cloning of pericentrin B. Thank you Jim for all the apple cakes that you always had handy for everybody's birthdays. I also would like to thank all my committee members for giving me advice and helpful feedback on my work. Finally, I would like to thank my family and friends for always being there for me, I could not have done it without you!

ABSTRACT

The work presented here describes novel functions for centrosome proteins, specifically for pericentrin and centriolin. The first chapter describes the involvement of pericentrin in ciliogenesis. Cells with reduced pericentrin levels were unable to form primary cilia in response to serum starvation. In addition we showed novel interactions between pericentrin, intraflagellar transport (IFT) proteins and polycystin 2 (PC2). Pericentrin was co-localized with IFT proteins and PC2 to the base of primary cilia and motile cilia. Ciliary function defects have been shown to be involved in many human diseases and IFT proteins and PC2 have been implicated in these diseases. We conclude that pericentrin is required for assembly of primary cilia possibly as an anchor for other proteins involved in primary cilia assembly. The second chapter describes identification of centriolin, a novel centriolar protein that localizes to subdistal appendages and is involved in cytokinesis and cell cycle progression. Depletion of centriolin leads to defects in the final stages of cytokinesis, where cells remain connected by thin intercellular bridges and are unable to complete abscission. The cytokinesis defects seemed to precede the G0/G1 p53 dependant cell cycle arrest. Finally, the third chapter is a continuation of the cytokinesis study and it identifies pericentrin as an interacting partner for centriolin. Like centriolin, pericentrin knockdown induces defects in the final stages of cytokinesis and leads to G0/G1 arrest. Moreover, pericentrin and centriolin interact biochemically and show codependency in their centrosome localization. We conclude that pericentrin and centriolin are members of the same pathway and are necessary for the final stages of cytokinesis.

TABLE OF CONTENTS

COPYRIGHT	ii
APPROVAL	iii
ACKNOWLEDGEMENTS	iv
ABSTRACT	v
TABLE OF CONTENTS	vi
LIST OF FIGURES	vii
LIST OF ABBREVIATIONS	viii
INTRODUCTION	1
CHAPTER I	16
CHAPTER II	39
CHAPTER III	79
DISCUSSION	100
REFERENCES	105

LIST OF FIGURES

FIGURE 1: Comparison of splice variants of pericentrin.	14
FIGURE 2: Pericentrin localizes to centrioles and basal bodies.	29
FIGURE 3: Pericentrin silencing inhibits primary cilia formation.	31
FIGURE 4: Localization of IFT proteins and PC2, and mislocalization of pericentrin in cells with reduced IFT20.	33
FIGURE 5: Pericentrin co-localizes to basal bodies with IFT proteins and PC2, and pericentrin silencing mislocalizes IFT proteins and PC2 from basal bodies and centrosomes.	35
FIGURE 6: Pericentrin interacts with proteins involved in cilia assembly and function.	37
FIGURE 7: Centriolin is a ~270-kDa coiled-coil protein localized to mature centrosomes and the midbody.	62
FIGURE 8: Centriolin is localized to maternal centrioles and noncentrosomal sites of microtubule anchoring.	65
FIGURE 9: RPE-1 cells treated with siRNAs targeting centriolin retain persistent intercellular connections and fail in cytokinesis.	67
FIGURE 10: Time-lapse images of HeLa cells treated with centriolin siRNAs reveal unique cytokinesis defects.	70
FIGURE 11: Cells expressing centriolin fail in cytokinesis, as do cells expressing the centriolin Nud1 domain that interacts with yeast Bub2p.	72

FIGURE 12: Cytokinesis failure in <i>Xenopus</i> embryos injected with centriolin Antibodies.	75
FIGURE 13: siRNAs targeting centriolin induces G1/G0 arrest.	77
FIGURE 14: Pericentrin B localization to the contractile ring and the midbody during cytokinesis.	88
FIGURE 15: Pericentrin B exhibits co-dependency with centriolin at the centrosome and co-localizes with it at the midbody.	90
FIGURE 16: Pericentrin and centriolin interact biochemically.	92
FIGURE 17: Pericentrin B co-localizes with endobrevin at the midbody ring during cytokinesis.	94
FIGURE 18: Pericentrin B RNAi induces a late stage cytokinesis defects.	96
FIGURE 19: Pericentrin B disruption causes G0/G1 arrest.	98

LIST OF ABBREVIATIONS

DHC1b – dynein heavy chain 1b

DIC – differential interference

γ -TURC – γ -tubulin ring complex

GCP2/3 – γ -tubulin complex proteins 2 and 3

IFT – intraflagellar transport

IP – immunoprecipitations

MEN – mitotic exit network

MKLP1 – M phase phosphoprotein 1

NEB – nuclear envelope breakdown

PCM – pericentriolar material

Pcnt – pericentrin

PC1/2 – polycystin 1 and 2 proteins

PKD1/2 – polycystic kidney disease genes 1 and 2

RPE1 – retinal pigmented epithelial cell line 1

SIN – septation initiation network

siRNA – small interfering RNA

SNARE – soluble N-ethylmaleimide-sensitive factor attachment protein receptor

TACC – transforming acidic coiled-coil protein

INTRODUCTION

Centrosome Structure and Functions

The centrosome is a tiny organelle approximately 1-2 μm in size located in the middle of most animal cells. Over a century ago, Boveri, described the centrosome as an intensely haematoxylin staining body surrounded by a radiating aster (Boveri, 1914). It is now known that the centrosome contains a pair of centrioles surrounded by a dense pericentriolar matrix from which the microtubules are nucleated. Like the DNA, the centrosome is duplicated once during the cell cycle in a semi conservative fashion. That is, the mother centriole maintaining its existing tubulin serves as a template for the newly generated one, which consists of both old and newly synthesized tubulin (Kochanski and Borisy, 1990). Centrosome duplication begins at the G1/S boundary and it is completed by mitosis when it serves as a spindle pole. As the cell completes mitosis each daughter cell acquires one centrosome (Reviewed by (Sluder and Hinchcliffe, 2000)).

The two centrioles of the centrosome are not identical and they are called mother and daughter. The mother centriole can be distinguished by two sets of nine appendages at its distal end that are responsible for the anchorage of astral microtubules (Bornens, 2002; Mogensen et al., 2000). A subset of centrosome proteins were localized to those appendages and they include ninein (Mogensen et al., 2000) and centriolin (Gromley et al., 2003). There are some cells that lack centrioles (higher plants, some meiotic cells

and embryonic systems) and these cells are able to organize acentriolar microtubule-organizing centers and a functional spindle, probably by using microtubule motors and structural proteins instead (Compton, 1998). When present, the centrioles act in dominant fashion to organize microtubules and spindles. The pericentriolar material (PCM) surrounds both centrioles forming an interconnected lattice like structure which provides a scaffold for proteins involved in microtubule nucleation (Dictenberg et al., 1998; Moritz et al., 1995a; Vogel et al., 1997). Microtubules are nucleated from the PCM by the small and large γ -tubulin ring complexes (γ -TuRC), both capable of nucleating microtubules (Zheng et al., 1995). Some organisms, like yeast, contain only the small complex (Knop et al., 1997), whereas higher organisms, like mammals, contain both complexes (Gunawardane et al., 2000; Murphy et al., 1998).

In addition to its role in microtubule organization and nucleation, in recent years, the centrosome was shown to play a very important role in cytokinesis, centriole duplication, cell cycle progression and ciliogenesis (Gromley et al., 2003; Hinchcliffe et al., 2001; Jurczyk et al., 2004; Keryer et al., 2003b; Khodjakov and Rieder, 2001). The best illustration of the importance of centrosome in cell cycle came from the experiments where centrosomes were removed either by microsurgery or laser ablation. Such cells were still able to organize spindles and undergo presumably normal mitosis. However, half of these cells had problems completing cytokinesis and subsequently they arrested in interphase of the next cell cycle (Hinchcliffe et al., 2001; Khodjakov and Rieder, 2001). Another study correlated the final events of cytokinesis with the movement of the

maternal centriole to the intracellular bridge, which was necessary for abscission (Piel et al., 2001). This idea came from budding yeast, where the spindle pole body (equivalent of the mammalian centrosome) has to move to the bud, bringing into contact the GDP-bound form of Tem1 and the guanine-nucleotide exchange factor, Lte1 to trigger cytokinesis and exit from mitosis (Bardin et al., 2000). Although the movement of the centriole in the last stages of cytokinesis is similar in yeast and mammalian systems, the molecular pathway in mammals has not been identified. Our work presented in chapter II (Gromley et al., 2003), identified centriolin as one of the possible molecular players in this process. Centriolin contains a domain that is homologous to yeast Nud1/Cdc11 proteins implicated in exit from cytokinesis (reviewed in (Hinchcliffe, 2003)). More work is necessary to identify additional molecular players if they are conserved between yeast and mammals.

Other structures associated with centrioles are centriolar satellites, which consist of electron-dense spherical granules, about 70-100 nm in diameter. They are localized around the centrosomes of many vertebrate cells and they can move along microtubules in a dynein-dependent way (Balczon et al., 1994; Dammermann and Merdes, 2002; Kubo et al., 1999). PCM-1 localizes to satellites and it was shown to control centrosome assembly and microtubule organization (Dammermann and Merdes, 2002).

Pericentrins

The centrosome proteins of pericentrin family are encoded by alternatively spliced products of one gene (Flory and Davis, 2003). Pericentrins are localized to the PCM (Doxsey et al., 1994; Flory and Davis, 2003), where they are transported on microtubules from the cytoplasm by the minus end directed motor, dynein, specifically through interactions with the dynein light intermediate chain (Purohit et al., 1999; Tynan et al., 2000). The best characterized isoforms of pericentrin include pericentrin A (approximately 250 kDa) and pericentrin B/kendrin (approximately 380 kDa) (Flory and Davis, 2003; Li et al., 2001). Pericentrin A is homologous to pericentrin B throughout the entire protein sequence (Flory et al., 2000) (Fig. 1). The C-terminus of pericentrin B is unique and it contains a calmodulin-binding region homologous to *S.cerevisiae* Spc110p, *S.pombe* Pcp1p (Flory et al., 2002; Flory et al., 2000), and *drosophila* PLP/CP309 (Kawaguchi and Zheng, 2003; Martinez-Compos et al., 2004). The yeast and *Drosophila* orthologs seem to be important for calmodulin-dependent attachment of γ -tubulin to the centrosome (Kawaguchi and Zheng, 2003; Knop and Schiebel, 1997; Nguyen et al., 1998; Sundberg et al., 1996). Pericentrin B, together with CG-NAP/AKAP450, seem to mediate this attachment in human cells (Takahashi et al., 2002). Although, recent data showed that pericentrin A can also mediate the attachment of γ -tubulin in human cells through its interactions with components of γ -tubulin ring complex proteins GCP2 and GCP3 (Zimmerman et al., 2004). The effect of pericentrins and its orthologs on microtubule nucleation and organization is controversial and probably depends on the level of protein depletion. In *Drosophila* both γ -tubulin and the

pericentrin B orthologue - CP309 are necessary for microtubule nucleation (Kawaguchi and Zheng, 2003). Specific depletion of pericentrin B had no effect on microtubule organization in mammalian cells (Li et al., 2001). However, *Xenopus* aster formation was inhibited with pericentrin B antibody (Takahashi et al., 2002) and a decrease in the density of nucleated microtubules in pericentrin B knockdowns was reported for pericentrin A and B depleted human cells (Dammermann and Merdes, 2002). Pericentrin A and B was shown to be important for spindle organization and function (Doxsey et al., 1994; Zimmerman et al., 2004). It was postulated that pericentrin B and CG-NAP/AKAP450 may play redundant roles in mammalian cells and that is why no effect on microtubule nucleation is observed when only one protein is depleted (Kawaguchi and Zheng, 2003). It is also possible that residual protein in the knockdowns is sufficient to sustain its activity or that different isoforms of pericentrin have specific and overlapping functions. More work needs to be done in order to fully understand the differences between pericentrin isoforms.

In addition to its role in microtubule and spindle function, pericentrin orthologue in *Drosophila* was shown to be important for cilia formation and function (Martinez-Compos et al., 2004). Other centrosome proteins including PCM-1 (Kubo et al., 1999), γ -tubulin (Muresan et al., 1993) and centrin (Gavet et al., 2003) have been localized to basal bodies, however their involvement in ciliogenesis has not been determined. Cilia play roles in motility and sensory reception. Their dysfunction contributes to cilia-related diseases and it will be discussed below.

Ciliogenesis

Cilia and flagella are specialized organelles which are anchored in the cell by the basal body and whose axonemes protrude from the cell surrounded by the plasma membrane of the cell (Rosenbaum and Witman, 2002). Cilia can be classified as motile or nonmotile based on their function. The motile cilia include flagella that propel cells and epithelial border cilia that beat synchronously and stir the extracellular fluid. Nonmotile cilia, also called primary or rudimentary, are found on almost every animal cell. The primary cilium of renal epithelial cells serve as a flow mechano-sensor, which bend in response to fluid flow and induces Ca^{2+} influx (Praetorius and Spring, 2001). Polycystin 1 (PC1) and 2 (PC2) co-localize to the cilia (Pazour et al., 2002b; Yoder et al., 2002) and function as mechanotransducers that increase intracellular calcium in response to fluid flow (McGrath et al., 2003; Nauli et al., 2003). PC1 and PC2 are gene products of (Polycystic Kidney Disease) PKD1 and PKD2, respectively, and they are mutated in polycystic kidney disease (Mochizuki et al., 1996). PC2 forms a complex with PC1 to generate a unique calcium-permeable channel (Hanaoka et al., 2000). Polycystin-mediated mechanotransduction is also necessary for the establishment of the left-right asymmetry of visceral organs in mouse embryos (McGrath et al., 2003). In this case, the cilia are located at the center of the node and produce movement that creates leftward fluid flow (McGrath et al., 2003). This nodal flow is critical for the asymmetric gene expression that establishes the left-right asymmetry (McGrath et al., 2003).

In terms of microtubule arrangement, nonmotile cilia are nonmotile because they are missing almost all structures other than the nine outer doublets (9+0 arrangement). Motile cilia contain the central pair of microtubules (9+2 arrangement) in addition to dynein arms. The centriole at the base of cilium is commonly referred to as the basal body and it grows satellites from its sides, a root from its base, and a cilium from its apex (Sorokin, 1968). The satellites and rootlets help to fix the position of the basal body beneath the cell surface. However, rootlets are frequently formed by motile cilia and rarely by primary cilia (Sorokin, 1968). The first steps in the formation of the cilium are characterized by the appearance of the vesicles at the distal end of a basal body and the ciliary bud beneath it (Sorokin, 1962). The vesicle then lengthened and fused with the plasma membrane (Sorokin, 1962).

The primary cilium arises directly off the microtubules of mother centriole, whereas motile cilia, such as the ones of the epithelial border of lungs, in addition to the centriole templated growth can also form from structures called 'deutrosomes' (Sorokin, 1968). Deutrosomes are electron dense structures that resemble centrioles and up to 14 procentrioles can assemble, regularly spaced, about one central deutrosome (Sorokin, 1968). Mature centrioles are then separated from deuterosomes and migrate toward the plasma membrane where they initiate cilia growth (Sorokin, 1968).

Intraflagellar Transport

Growth of the ciliary fiber occurs at the tips and axoneme subunits are delivered to the tips by a process called intraflagellar transport (IFT). This transport was first observed a decade ago in the green alga *Chlamydomonas* at the laboratory of Joel Rosenbaum at Yale (Kozminski et al., 1993). IFT carries protein particles between the outer doublet microtubules and the membrane of flagella or cilia and it has been described in many organisms including *Chlamydomonas*, *Tetrahymena*, *C. elegans*, sea urchin and mouse (Rosenbaum, 2002; Rosenbaum and Witman, 2002). The IFT particle consists of two protein complexes, complex A (550 kDa) and complex B (710-760 kDa) (Cole et al., 1998; Piperno et al., 1998). The relationship between complex A and B are not clear. It was postulated that complex B proteins may be involved with anterograde transport (toward the tip of cilia) and flagellar assembly and complex A proteins in retrograde IFT (from the tip to basal body) (Scholey, 2003). All of the pericentrin-IFT interactions presented in chapter I include members of the complex B. The particles are moved to the tip of the cilia by a plus-end-directed motor, kinesin-II (Kozminski et al., 1995; Walther et al., 1994). Mutants with defects in kinesin-II were shown to lose their flagella when shifted to restrictive temperature (Walther et al., 1994). The retrograde movement of particles along the cilia is supported by cytoplasmic dynein 1b (Pazour et al., 1998; Porter et al., 1999) (reviewed in (Rosenbaum and Witman, 2002)). *Chlamydomonas* with a deletion of DHC1b had short flagella filled with IFT proteins (Pazour et al., 1999).

Mutations in IFT complex A or B or either one of the IFT motor complexes result in cells that lack flagella or have short, defective flagella. For example, inducible RNAi of IFT proteins in *Trypanosomes* leads to the assembly of a shorter flagellum, that is proportional to smaller cell size (Kohl et al., 2003). In this study the IFT depletion had an effect only on the newly formed flagellum, the older one was not affected. This is in agreement with earlier reports demonstrating that ciliary microtubules are stable structures which are able to withstand treatment by both nocodazole and colchicine, and are not in a dynamic equilibrium with cytoplasmic subunits (Tilney and Gibbins, 1968). However, more recently it has been shown that flagellar axonemal microtubules in sea urchin, *Chlamydomonas* and sensory cilia in *C. elegans* are dynamic structures (Fujiwara et al., 1999; Song and Dentler, 2001; Stephens, 1997; Stephens, 2000). The effect of IFT protein depletion on cilia length was also seen in many organisms including *Trypanosomes* (Kohl et al., 2003), *Chlamydomonas* (Brazelton et al., 2001; Kozminski et al., 1995), mouse (Murcia et al., 2000; Pazour et al., 2000), *C. elegans* (Cole et al., 1998; Perkins et al., 1986), and humans (Pazour IFT20 unpublished data).

In mammalian systems, defects in the IFT process as well as polycystins are associated with polycystic kidney disease (Pazour and Rosenbaum, 2002). The *Chlamydomonas* IFT88 orthologue in the mouse encoded by the *Tg737* gene when mutated leads to autosomal recessive polycystic kidney disease (Moyer et al., 1994). In addition, the mouse *Tg737* gene product, *polaris*, when mutated shows defects in assembly of the primary cilia in kidney (Pazour et al., 2000). One of the features connecting both IFT

and polycystin models of the kidney disease is defective or inconspicuous cilia (Pazour et al., 2000; Thomson et al., 2003). Moreover, PC2 was shown to localize to the primary cilia on kidney cells (Pazour et al., 2002b) and since cilia are not present (or are truncated) in the IFT88/polaris mutants, this suggests that functional PC2 containing ion channels are also not assembled. Taken together, these observations suggest that kidney primary cilia are important for proper kidney cell function and defects in the primary cilia can lead to polycystic kidney disease.

Cytokinesis

Cytokinesis is defined as division of cytoplasm into two daughter cells following mitosis. This process begins in anaphase with furrow ingression which proceeds until the cytoplasm is constricted to a narrow bridge called midbody. The final stages of cytokinesis consist of resolution of the midbody and abscission resulting in two daughter cells. The cleavage furrow regression occurs as a result of construction of actomyosin ring, which is composed of actin and myosin II (Carter, 1967; Fujiwara et al., 1978). The mechanism by which abscission is completed remains largely unknown. Chromosome passenger proteins have been shown to be important for cytokinesis, since their disruption leads to cytokinesis failure resulting in multinucleated cells (Adams et al., 2001; Bischoff and Plowman, 1999; Carvalho et al., 2003; Gassmann et al., 2004; Lens et al., 2003; Li et al., 1999; Mackay et al., 1998; Romano et al., 2003; Sampath et al., 2004; Vagnarelli and Earnshaw, 2004).

After mitotic cells have been nearly separated by the ingression of contractile ring the final separation of the two daughter cells requires a number of proteins and events. The proteins implicated in the final stages of cytokinesis include members of vesicular trafficking and membrane fusion. Vesicle fusion has been well characterized in plant cell division where a structure called the phragmoplast is formed in the middle of the cell by targeted secretion of post-golgi vesicles. Moreover, *C.elegans* embryos show defects in late stages of cytokinesis upon treatment with brefeldin A, which inhibits post-golgi vesicle secretion (Skop et al., 2001).

More recent studies in mammalian cells of the SNARE (Soluble N-ethylmaleimide-sensitive factor Attachment protein REceptor) complex showed the importance of vesicle fusion during cytokinesis (Low et al., 2003). Overexpression of the components of SNARE complex, specifically syntaxin-2 or endobrevin, result in cytokinesis failure and formation of binucleate cells. This complex of protein mediates the fusion of vesicles and its target membrane (Jahn and Sudhof, 1999). Completion of the late events of cytokinesis also requires septins (Field and Kellogg, 1999). One of the members of septin complex, CDCrel-1 was shown to interact with the syntaxin, t-SNARE protein (Beites et al., 1999). Thus, septin complexes may also facilitate the cytokinesis by mediating the daughter cells membrane fusion (reviewed in (Schweitzer and D'Souza-Schorey, 2004)).

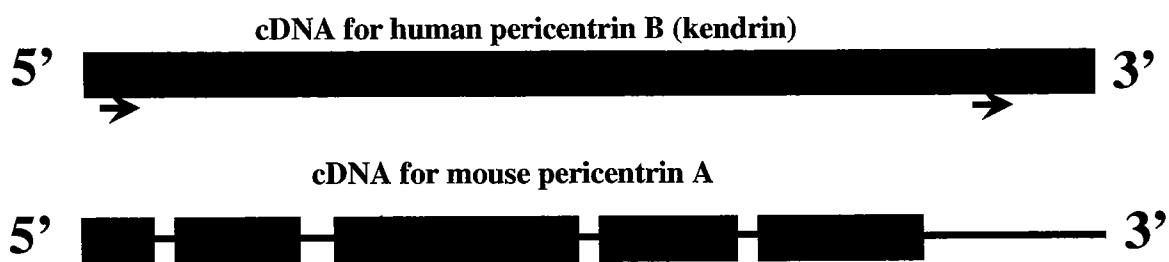
Studies in both the budding and fission yeast implicated the involvement of exocyst complex in cytokinesis. Exocyst complex is known to target secretory vesicles to their site of secretion (Hsu et al., 2004; Wang et al., 2004). In the budding yeast, members of the exocyst complex are localized to the mother-bud neck suggesting a role in cytokinesis (Finger et al., 1998). Cells overexpressing the exocyst component SEC15 accumulate vesicles at the site of cytokinesis in *S. cerevisiae* (Salminen and Novick, 1989). In *S. pombe* the exocyst components are also localized to the site of cytokinesis. Moreover, the exocyst mutants accumulate vesicles at the septum and are defective in cleaving the cells (Wang et al., 2002a).

Kinesin-related proteins, CHO1/MKLP1 (**Mitotic Kinase-Like Protein 1**), RAB6-KIFL, and MPPI (**M Phase Phosphoprotein 1**) are also essential for cytokinesis. Centralspindlin complex consisting of MKLP-1/CHO1 and the GTPase Activation Protein (GAP), was shown to form a ring inside the actomyosin contractile ring, which controls furrow ingression by regulation of the GTPase RhoA protein (Saint and Somers, 2003). CHO1/MKLP1 was also shown to block mitotic progression (Nislow et al., 1990) in addition to disrupting the microtubule bundling at the midzone (Matuliene and Kuriyama, 2002). RAB6-KIFL was necessary for the final stages of cytokinesis (Fontijn et al., 2001; Hill et al., 2000). Overexpression of RAB6-KIFL resulted in cell death and cells connected by a midbody remnant (Hill et al., 2000). In addition, antibody injection experiments lead to failure in cytokinesis after cleavage furrow ingression. RNA interference of MPP1 resulted in cytokinesis failure followed by apoptosis (Abaza et al.,

2003). How the kinases function to regulate cytokinesis is not known, however, CHO1/MKLP1 was shown to bind the ARF GTPases, which are involved in endosomal cycling (Boman et al., 1999; Schweitzer and D'Souza-Schorey, 2002). Therefore, membrane vesicle trafficking could be one way to facilitate daughter membrane fusion events.

Figure 1. Comparison of splice variants of pericentrin. Pericentrin B also known as kendrin is a bigger isoform (~380 kDa) and pericentrin A is a smaller isoform (~250 kDa). Boxes indicate exons present in both pericentrin A and B and lines indicate the location of exons present in pericentrin B but not in pericentrin A. Arrow heads on pericentrin B indicate the positions of the siRNAs targets used for silencing.

FIGURE 1



Chapter I

Pericentrin Forms a Complex with Intraflagellar Transport Proteins and Polycystin 2 and is required for Primary Cilia Assembly

Abstract

Primary cilia are nonmotile microtubule structures that assemble from basal bodies by a process called intraflagellar transport (IFT) and are associated with several human diseases. Here we show that the centrosome protein pericentrin co-localizes with IFT proteins to the base of primary and motile cilia. Immunogold electron microscopy demonstrates that pericentrin is on or near basal bodies at the base of cilia. Pericentrin depletion by RNA interference disrupts basal body localization of IFT proteins and the cation channel polycystin-2 (PC2), and inhibits primary cilia assembly in human epithelial cells. In addition silencing of several other centrosome proteins including PCM-1 and members of the γ -tubulin ring complex proteins were able to inhibit primary cilia formation. Ninein was the only centrosome protein that when silenced did not inhibit primary cilia formation. Conversely, silencing of IFT20 mislocalizes pericentrin from basal bodies and inhibits primary cilia assembly. Pericentrin is found in spermatocyte IFT fractions, and IFT proteins are found in isolated centrosome fractions. Pericentrin antibodies co-immunoprecipitate IFT proteins and PC2 from several cell lines and tissues. We conclude that pericentrin, IFTs and PC2 form a complex in vertebrate cells that is required for assembly of primary cilia and possibly motile cilia and flagella.

Introduction

Centrosomes serve as microtubule organizing centers in interphase and mitotic cells and play a role in cytokinesis and cell cycle progression (Doxsey, 2001). They are also the precursors of primary cilia, nonmotile sensory organelles found on most vertebrate cells. Ciliary dysfunctions are associated with several human diseases (Pazour and Rosenbaum, 2002; Rosenbaum and Witman, 2002). Primary cilia in vertebrate cells appear to arise from the mother centriole of the centrosome within a membrane sheath, which forms from cytoplasmic vesicles and ultimately fuses with the plasma membrane (Sorokin, 1968). The intimate relationship between the centrosome and the primary cilium suggests that functions and components may be shared between these structures.

Primary cilia assembly occurs by a process called intraflagellar transport (IFT) (Han et al., 2003; Kozminski et al., 1993; Pazour and Rosenbaum, 2002; Rosenbaum, 2002; Rosenbaum and Witman, 2002). Interference with IFT protein function results in loss or reduction of primary cilia (Pazour et al., 2002a; Pazour et al., 2000; Pazour and Rosenbaum, 2002). Primary cilia possess cation channels and receptors that appear to activate signal transduction pathways that control cellular function (Pazour et al., 2002a; Pazour and Rosenbaum, 2002; Pazour and Witman, 2003). PC2 is a calcium-selective channel on primary cilia associated with polycystic kidney disease (Somlo and Ehrlich, 2001). It appears to be activated by mechanical movement of primary cilia in response to fluid flow (Nauli et al., 2003) and controls the assembly of primary cilia (Thomson et al.,

2003; Watnick et al., 2003). However, little is known about the mechanism by which IFT proteins and PC2 are organized at the centrioles/basal bodies (terms used interchangeably).

A role for centrosome proteins in primary cilia formation has recently been established. Mutants of a *Drosophila* protein that shares homology with the vertebrate centrosome proteins pericentrin (Pcnt) (Flory and Davis, 2003; Zimmerman et al., 2004) and AKAP450 (Keryer et al., 2003a) disrupt formation of mechanosensory and chemosensory cilia (Martinez-Compos et al., 2004). *Drosophila* mutants that affect IFT also disrupt formation of *Drosophila* sensory cilia (Han et al., 2003). However, the molecular mechanism by which centrosomes and centrosome proteins modulate primary cilia assembly has not been determined. In this study, we show that Pcnt forms a complex with IFT proteins and PC2 in vertebrate cells and tissues, and that Pcnt depletion by small interfering RNAs (siRNA) disrupts centriole association of IFTs and PC2 and inhibits primary cilia formation.

Results and Discussion

In this study, we have studied a larger isoform of Pcnt using specific siRNAs and antibodies unless otherwise noted (Flory and Davis, 2003; Zimmerman et al., 2004). Immunofluorescence imaging demonstrated that Pcnt partially overlapped with centriolin, a protein associated with the mother centriole at centrosomes (Fig. 2 a) (Gromley et al., 2003). In addition, Pcnt associated with both centrioles at the base of

primary cilia (Fig. 2 b-c) and motile cilia (Fig. 2 d). Higher resolution immunogold electron microscopy demonstrated that Pcnt was on or near the centrioles of motile cilia (Fig. 2 e).

To test the role of Pcnt in cilia organization we depleted protein levels by siRNA. We observed a 75-90% reduction in protein levels and a dramatic reduction in centrosome levels of Pcnt in most cells (Fig. 3 a-c, arrow in c), when compared with cells treated with control siRNAs targeting lamins A/C (Fig. 3 a-b) or cells that did not respond to siRNA treatment (Fig. 3 c, lower cell). In contrast, centrosome localization of γ tubulin was only slightly affected under these conditions (Fig. 3 c, upper cell). Primary cilia were induced in RPE1 cells treated with siRNAs targeting Pcnt and were detected with antibodies to polyglutamylated tubulins (GT335) (Gromley et al., 2003) and by differential interference microscopy (DIC). In most cells treated with siRNAs targeting Pcnt, primary cilia failed to assemble (Fig. 3 e, g, h), while control cells treated with siRNAs targeting lamin or ninein assembled normal full-length primary cilia (Fig. 3 d, f, h). In addition silencing of other centrosome proteins including centriolin, γ -tubulin, PCM-1 and centrin also inhibited the primary cilia formation (Fig. 3 h).

To address the mechanism of ciliary loss in cells with reduced Pcnt, we examined centriole function, structure and composition. Consistent with previous results from our group and others (Dammermann and Merdes, 2002; Martinez-Compos et al., 2004; Zimmerman et al., 2004), we found that microtubule organization and nucleation were

not significantly disrupted. In addition, centriole ultrastructure was normal (Fig. 3 i-k, n = 45 centrosomes). Centrioles were sometimes separated (Fig. 3 e, g), but this was also observed following functional abrogation of proteins that did not affect primary cilia (e.g. ninein).

Since vertebrate primary cilia formation and function requires IFT proteins (Murcia et al., 2000; Pazour et al., 2000) and the cation channel PC2 (Nauli et al., 2003; Pazour et al., 2002b; Rosenbaum and Witman, 2002; Somlo and Ehrlich, 2001), we reasoned that Pcnt might cooperate with these proteins in primary cilia organization. To test this, we first determined the precise localization of these proteins. IFT57 and IFT88 localized primarily to the distal end of the mother centriole near the base of the primary cilium and to the tips and in spots along the length of primary cilia (Fig. 4 a-b). Localization of these IFTs to the distal portion of the mother centriole was consistent with known sites of IFT protein localization in *Chlamydomonas reinhardtii* (Cole et al., 1998; Deane et al., 2001). IFT20 was found on the proximal portion of mother centriole and the lateral aspect of the daughter centriole (Fig. 4 c), an area thought to be involved in interconnecting the two centrioles. PC2 localized primarily to the mother centriole underlying the primary cilium (Fig. 4 d). In mouse tracheal epithelial cells, IFT proteins partially localized with Pcnt to sites at the base of the motile cilia where basal bodies are found (Fig. 4 e, IFT20).

We next addressed the centriolar anchoring mechanism of Pcnt, IFTs and PC2. We found that Pcnt was dependent on IFT proteins for localization to basal bodies using cells that

stably express siRNAs targeting IFT20 (Follit and Pazour, unpublished observations). These cells showed reduced centriolar IFT20 and lacked primary cilia (Fig. 4 g-g'', h), compared with cells of the parent line (Fig. 4 f-f'', h). In cells with reduced centriole-associated IFT20, we observed a similar reduction in Pcnt levels (Fig. 4 g, g'', i). In a reciprocal experiment, we found that IFTs and PC2 were dependent on Pcnt for centriole localization. Pcnt localized to both centrioles at the base of cilia, partially co-localized with IFT proteins (Fig. 5 a'', IFT57) and totally overlapped with PC2 (Fig. 5 c''). Pcnt silencing reduced the levels of centriolar Pcnt (Fig. 5 b, b'', c, c'' upper cell), IFT57 (Fig. 5 b'-b'') and PC2 (Fig. 4 c'-c'' upper cell). In contrast, adjacent nontransfected cells or cells treated with lamin siRNAs had robust staining for IFT57 and PC2 (Fig. 5 a'-a'', c'-c'' lower cell). These results show that Pcnt and IFTs are co-dependent in their localization to basal bodies of primary cilia.

Previous studies showed that IFT protein complexes and Pcnt complexes had similar S values on sucrose gradients (17-18S) (Dictenberg et al., 1998; Pazour et al., 2002a). To determine whether Pcnt interacted with IFT proteins, we isolated IFT complexes by a multistep procedure (San Agustin and Witman, 2001) and found that Pcnt A and B appeared to be in the same fractions with IFT88 in the final gel filtration column (Fig. 6 a). Based on recent data showing that IFT71 is present on centrosomes and spindle poles (Iomini et al., 2004), we analyzed centrosome preparations (Doxsey et al., 1994) for the presence of IFT proteins. IFT88 (Fig. 6 b) were present in pooled fractions containing centrosome proteins (γ tubulin, Pcnt) but not in pooled fractions lacking centrosomes.

Immunoprecipitation of Pcnt using antibodies (that recognize both small, Pcnt A and large, Pcnt B isoforms) raised to two independent domains pulled down endogenous IFT88 from two ciliated cell lines (Fig. 6 c, two upper panels), ectopically expressed GST-GFP-IFT20 (Fig. 6 c, lower panel) and endogenous PC2 from mitotic cells (Fig. 6 d). We observed no co-immunoprecipitation of any IFT protein or PC2 when Pcnt antibody was omitted (Fig. 6 d, Bd) or substituted with a nonimmune IgG (Fig. 6 c, e, IgG). α -tubulin antibody (dM1 α) was used as negative control for pcnt immunoprecipitation. We observed no co-immunoprecipitation of α -tubulin with pcnt and in the same immunoprecipitation reactions we were able to pull down endogenous IFT88 and pcnt (Fig. 6 f). In reciprocal experiments, we found that PC2 immunoprecipitation pulled down endogenous IFT57 from ciliated cells (Fig. 6 e) and that IFT57 pulled down IFT88 (Fig. 6 c). Taken together, these biochemical data suggest that Pcnt, PC2 and IFT proteins form a complex in the cytoplasm of vertebrate cells.

The data in this manuscript show that Pcnt binds IFT proteins and PC2 and is required for primary cilia formation in human cells. This suggests a model in which Pcnt recruits protein complexes involved in cilia assembly and calcium signaling to centrioles at the base of primary cilia (and perhaps flagella). Since *Drosophila* Pcnt/AKAP450 and IFT were shown separately to function in primary cilia assembly (Han et al., 2003), it is possible that Pcnt has a conserved function in IFT organization during cilia formation in both *Drosophila* and vertebrate cells.

IFT does not appear to play a role in assembly or function of *Drosophila* sperm flagella (Han et al., 2003) as seen in other organisms (Rosenbaum and Witman, 2002). Thus, it is unlikely that defects in flagellar motility in *Drosophila* Pcnt/AKAP450 mutants (Martinez-Compos et al., 2004) are a consequence of disruption of the Pcnt-IFT interaction. However, both vertebrate Pcnt (Dictenberg et al., 1998; Takahashi et al., 2002; Zimmerman et al., 2004) and *Drosophila* Pcnt/AKAP450 (Kawaguchi et al., 2003) interact with complexes containing γ tubulin, and γ tubulin has recently been shown to be required for flagellar motility in trypanosomes (McKean et al., 2003). Thus, it is possible that disruption of the interaction between Pcnt/AKAP450 and γ tubulin complexes could account for lack of motility in *Drosophila* flagella. Another possibility is that the observed structural alterations in centrioles in spermatocytes from *Drosophila* Pcnt/AKAP450 mutants (Martinez-Campos et al., 2004) could contribute to defects in both cilia and flagella. However, in this study we did not detect changes in centriole structure in cells depleted of Pcnt. Given the recent findings that Pcnt and other centrosome proteins are integral components of cilia and flagella and that IFT proteins and PC2 are integral components of centrosomes and spindle poles (Iomini et al., 2004) it is likely that perturbation of proteins in one of these compartments affects the function of the other. Since defects in centrosome and spindle pole are well documented in cells with abrogated Pcnt and Pcnt orthologs, they could contribute to defects in centrosome derivatives such as cilia and flagella. It is clear from this discussion that a better

understanding of the precise role of Pcnt in cilia and flagella assembly/function will require additional studies.

On a final note, it is interesting that centrosomes in *Drosophila* Pcnt/AKAP450 mutants are disorganized but appear to assemble normal mitotic spindles (Martinez-Compos et al., 2004). It is possible that residual functional protein remaining in *Drosophila* mutants is sufficient for spindle function. However, recent results from vertebrate cells indicate that there are several forms of Pcnt (Floury and Davis, 2003), and that a smaller form of the protein is required for spindle organization and function, possibly through its role in anchoring γ tubulin complexes or IFT proteins at spindle poles (Zimmerman et al., 2004). A larger Pcnt isoform that shares homology with *Drosophila* Pcnt/AKAP450 does not have a dramatic effect on spindle organization (Zimmerman et al., 2004). It is likely that the multiple Pcnt isoforms contribute to a multitude of cellular functions.

Materials and methods

Cells, siRNAs, IFT isolation and primary cilia formation

Cells used in this study, RPE1 (Morales et al., 1999), a mouse inner medullar collecting duct (IMCD3), primary cells isolated from Tg737 wild type mouse (488) (Pazour et al., 2000) and freshly-isolated primary mouse trachea cells, were grown as described in ATCC. Trachea dissected from mice in PBS were opened and scraped with a wooden applicator stick. Released ciliated epithelial cells were spun onto cover slips and fixed in -20°C methanol. siRNAs (21-nucleotide, Dharma on Research, Inc.) targeting Pcnt B (Gene Bank Acc. No. XM_036857,

nucleotides 301-319), Pcnt A/B or ninein (Dammermann and Merdes, 2002) and lamin A/C (Gromley et al., 2003), were delivered to cells at 200 nM (Oligofectamine, Invitrogen). We also used a stable RPE1 cell line expressing IFT20-specific siRNAs (GGAAGAGTGCAAAGACTTT) (Follit and Pazour, in preparation).

IFT protein fractions were prepared as described (San Agustin and Witman, 2001) using additional protease inhibitors A (Complete Mini tablets, Roche Diagnostics, Mannheim Germany) in lysis buffer. The two testes were homogenized in 500 μ l of modified homogenization buffer (35 mM NaHCO₃, 2 mM Na₂HPO₄, 70 mM KCl, 74 mM NaCl [McGrady, 1979], 1 mM DTT, 0.16% digitonin, 10 mM 4-aminobenzamidine, 2 mM EDTA, 50 μ M leupeptin, 15 μ M pepstatin, 100 μ M TLCK, 1 μ g/ml aprotinin, Complete protease inhibitor cocktail tablet [Sigma], pH 6.9). The clarified testis extract was layered on top of a 12-ml 5-20% sucrose gradient that had the same buffer composition as the homogenization buffer but without digitonin, and then centrifuged in a Beckman L5-75 ultracentrifuge (36,000 rpm, SW41 rotor, 4 °C). The cumulative centrifugal effect (ω^2t) was set at 6.4×10^{11} radians²/sec. About 24 fractions (500 μ l each) were then collected, electrophoresed in SDS-PAGE gels, transferred to PVDF membranes and probed with anti-IFT antibodies. IFT-containing sucrose gradient fractions of testis extracts from 6 mice were pooled, concentrated (Centriplus 10, Amicon), and applied to a Superose 6 column (HR 10X30, AP Biotech,) that had been equilibrated with column buffer (30 mM Na₂CO₃, 2 mM NaH₂PO₄, pH 6.9, 78 mM KCl, 70 mM NaCl, 2 mM EDTA, 1 mM DTT). Fractionation flow rate was 0.2 ml/min. Fractions (500 μ l) were collected, electrophoresed in 5%

SDS-PAGE gels, transferred to PVDF membranes, and probed with anti-pericentrin and anti IFT88 antibodies.

Primary cilia were induced following siRNA treatment (72 hours) by culturing RPE1 cells in medium with 0.25% serum and siRNAs for 48 h and identified using GT335 antibody and DIC microscopy.

Immunofluorescence, electron microscopy and RT-PCR

Cells were prepared for immunofluorescence, imaged, deconvolved (Metamorph; Universal Imaging Corp.) and displayed as two-dimensional projections of three-dimensional reconstructions to visualize the entire cell volume as described in (Gromley et al., 2003). We used methanol as fixative, then confirmed using formaldehyde fixation as previously shown (Dictenberg et al., 1998). Immunogold electron microscopy was performed as described (Doxsey et al., 1994). RT-PCR for amplification of Pcnt B (forward primer 5'-AACACTCTCCATGATTGCC and reverse 5'-TACCCTCCCAATCTTTGCTG) and α tubulin was performed as described (Gromley et al., 2003).

Immunoprecipitation, Western Blotting and Antibodies

Cells were lysed in lysis buffer consisting of 50mM Tris HCl (pH 7.5), 10 mM Na₂HPO₄ (pH 7.2), 1 mM EDTA, 150 mM NaCl, 1% IGEPAL CA-1630 and Complete Mini tablets. Testes lysates were prepared as described (San Agustin and Witman, 2001).

Antibodies were added to freshly prepared cell extracts and incubated at 4⁰C overnight. Protein A/G Plus-Agarose (Santa Cruz Biotechnology) or Glutathione Sepharose 4B (Amersham Pharmacia Biotech AB, Upsala Sweden) were washed in lysis buffer, added to the cell extracts and incubated 2 h at 4⁰C. The beads were washed and resuspended in sample buffer. 5% SDS-PAGE gels were used to detect Pcnt and PC2, 10 % gels to detect IFTs. Controls included cell extracts incubated with rabbit IgG or beads alone. No bands were seen with control IgGs under any of these conditions or when control IgGs were used at concentrations > 10-fold higher than experimental samples. Cell extracts used in this study for the pericentrin IFT interactions came from cells grown in 0.25% serum for 48 h to induce cilia formation. We used affinity-purified antibodies against: the N- and C- termini of Pcnt A/B (PcN, PcC) (Dictenberg et al., 1998; Doxsey et al., 1994), Pcnt B (Flory et al., 2000), IFT proteins (Pazour et al., 2002a), PC2 (Scheffers et al., 2002), centriolin (Gromley et al., 2003), GT335 (Wolff et al., 1992), α tubulin (Sigma-Aldrich), and lamin A/C (Cell Signaling Technology).

Figure 2. Pericentrin localizes to centrioles and basal bodies. (a)

Immunofluorescence image of a centrosome in RPE1 cells co-stained for Pcnt (green) and centriolin (red, bar, 1 μm). (b, c) DIC (b) and immunofluorescence (c) images of a primary cilium (arrow) in RPE1 cell stained for Pcnt (green) and centrioles/primary cilium (GT335, red). Bar, 5 μm for b, c. (d) Immunofluorescence image of a ciliated epithelial cell from mouse trachea showing Pcnt (green) at the base of motile cilia (DIC, bar, 5 μm). (e) Immunogold electron microscopic image of a ciliated cell (as in d) after incubation with antibodies to Pcnt and secondary antibodies bound to 5 nm gold (bar, 250 nm). Stephen Doxsey contributed the pericentrin electron microscopic image and Agata Jurczyk contributed the rest.

FIGURE 2

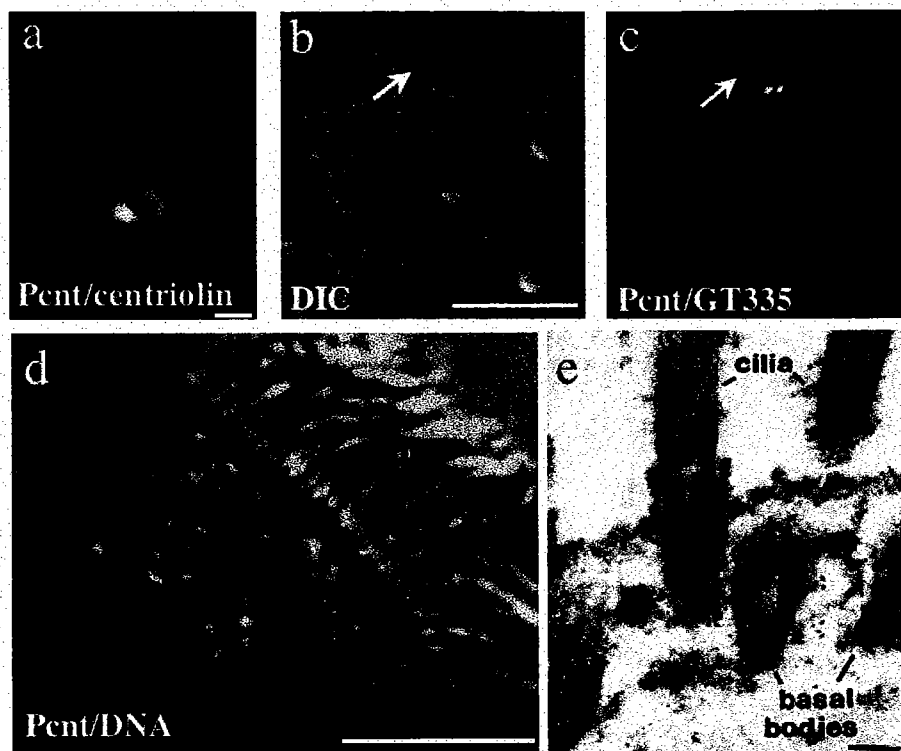


Figure 3. Pcnt silencing inhibits primary cilia formation. (a) Pcnt and lamin protein levels (a, Western blot) following siRNA as indicated. α tubulin or PKC, loading controls. (b) Fluorescence intensity of individual centrosomes (bars) after treatment with siRNAs targeting Pcnt or lamin. Centrosomal Pcnt is reduced to levels below the lowest control levels (lamin) in 87% of cells. (c) Immunofluorescence image of RPE1 cells after Pcnt silencing showing reduced centrosomal Pcnt in one cell (green, arrow) and normal level in the other. γ tubulin (red) is not significantly affected. Low (d, e) and high magnification (f, g) immunofluorescence images of cilia and centrioles stained with GT335 after treatment with Pcnt (e, g) or lamin (d, f) siRNAs. Bar in e, 5 μ m for d, e, or in f, 1 μ m for f, g. DNA, blue. (h) Graph showing percent of cells that lack cilia after treatment with indicated siRNAs. Bars represent average of 3 experiments. P value, standard T-test. (i-k) Electron micrographs showing centriole structure in cells with reduced Pcnt (bar in k, 200 nm for i-k). Gregory Hendricks did the electron microscopy for figures 3 i-k and Agata Jurczyk contributed the rest.

FIGURE 3

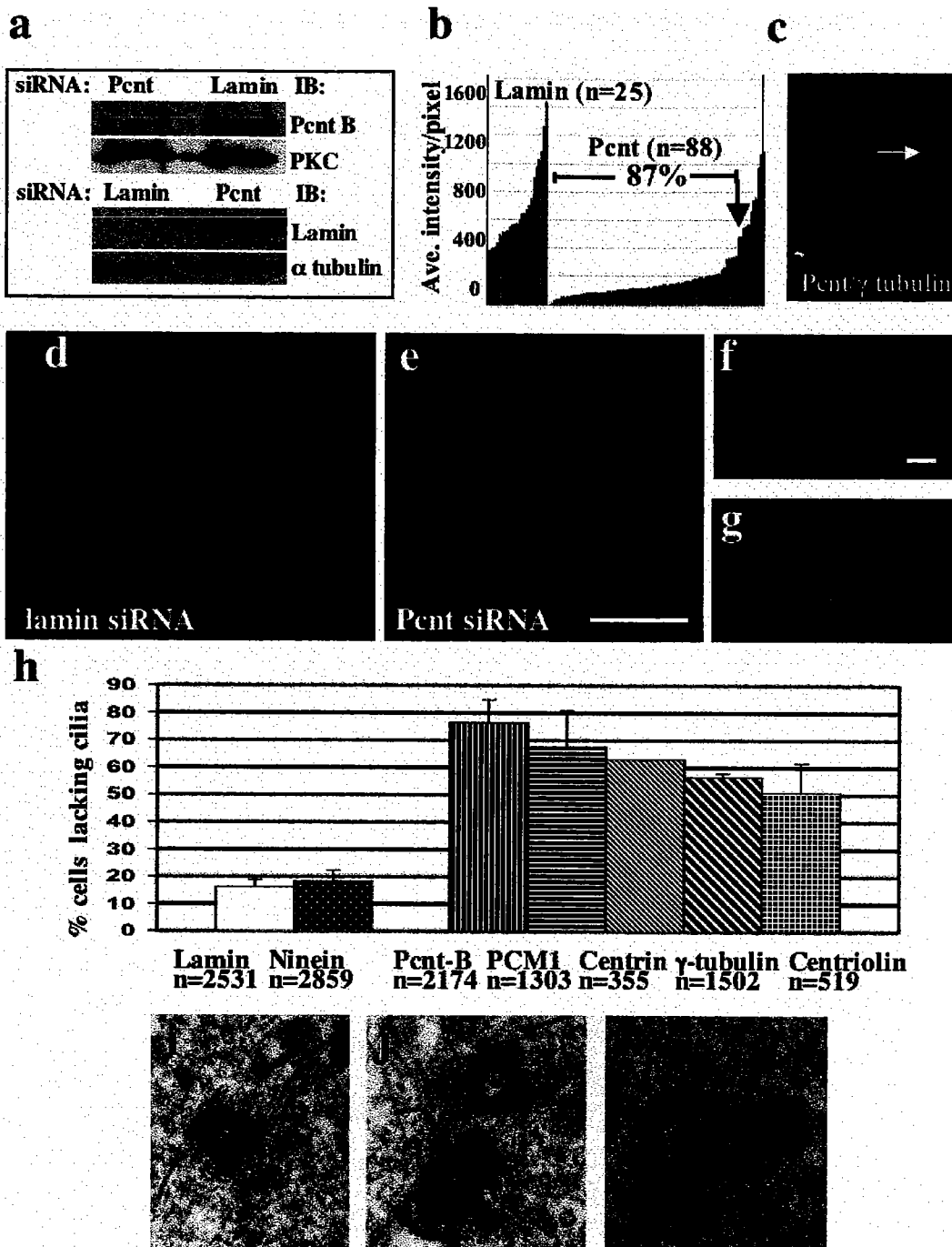


Figure 4. Localization of IFT proteins and PC2, and mislocalization of Pcnt in cells with reduced IFT20. (a-d) RPE1 cells stained for IFT57, IFT88, IFT20 and PC2 (green) and for basal bodies/cilia (GT335, red), Bar in d, 1 μm . (e) Pcnt (green) partially co-localizes with IFT20 (red) at the base of motile cilia (seen by DIC) in mouse epithelial cells. DNA, blue, bar, 5 μm . (f-g'') Untreated RPE1 cells (f-f'') or RPE1 cells stably expressing siRNA targeting IFT20 (g-g'') showing centrosomal levels of IFT20 (f'g'), Pcnt (f, g, bar, 5 μm) or merge (f'', g'', Pcnt, red, IFT20, green, DNA, blue at arrows. Insets, enlargements of f'', g''. (h-i) Fluorescence intensity of IFT20 (h) and Pcnt (i) at individual centrosomes (bars) in cells stably expressing IFT20 siRNA or mock, as indicated below graph. Stephen Doxsey and Sambra Redick contributed to figure 4 e and Agata Jurczyk contributed the rest.

FIGURE 4

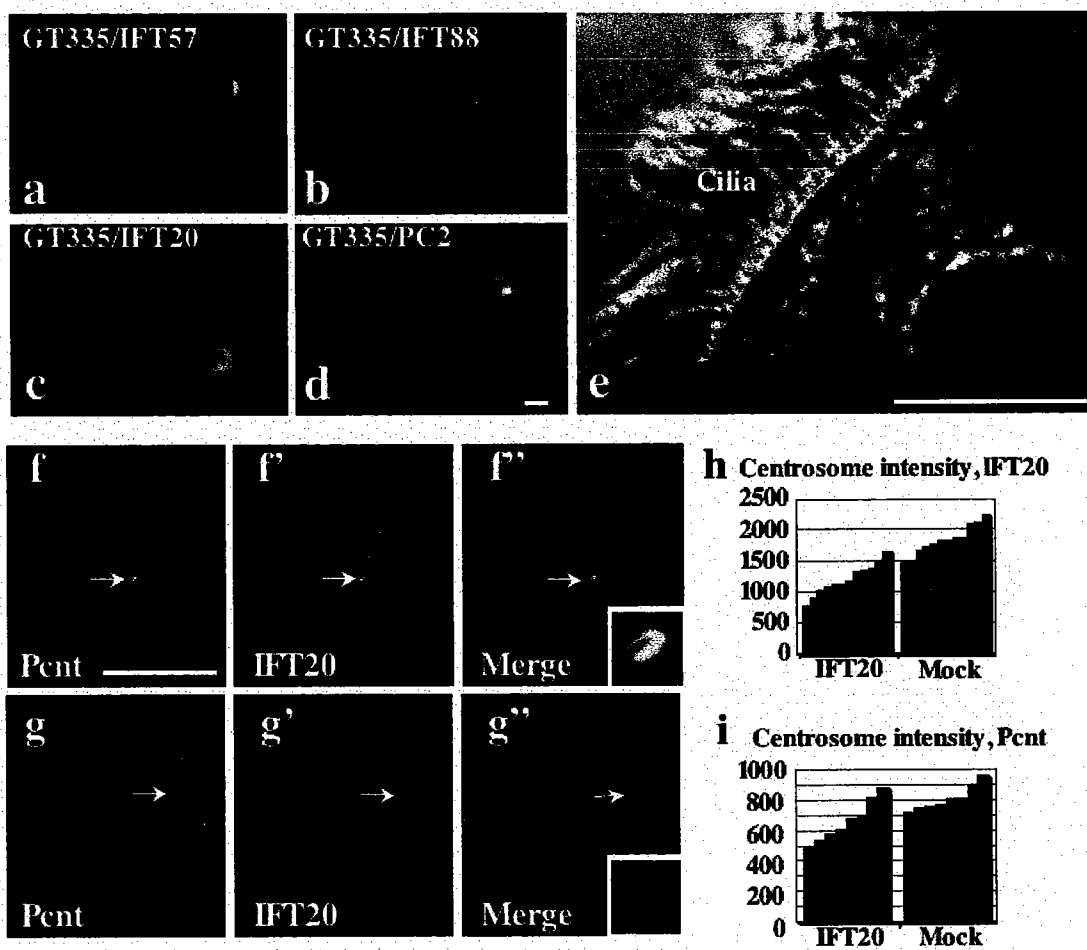


Figure 5. Pcnt co-localizes to basal bodies with IFT proteins and PC2, and Pcnt silencing mislocalizes IFT proteins and PC2 from basal bodies and centrosomes. (a-c'') IFT57 (a-b'' red) and PC2 (c-c'', red) are mislocalized from basal bodies in RPE1 cells with reduced Pcnt (b-b'', arrows, c-c'', green, small arrows) but not in RPE1 cells treated with lamin siRNAs (a-a'', bar, 10 μ m) or in the cell with control level of Pcnt (c, c'', bottom). Insets higher magnification of a'', b'', c'' as indicated by arrows. DNA, blue. Agata Jurczyk contributed the entire figure.

FIGURE 5

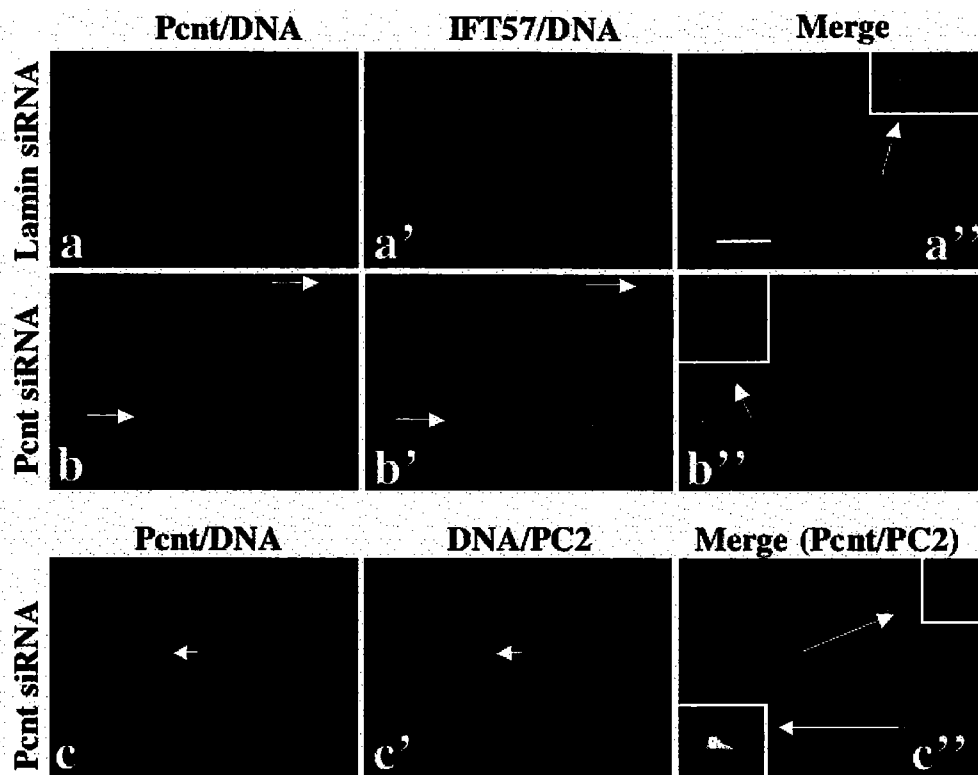
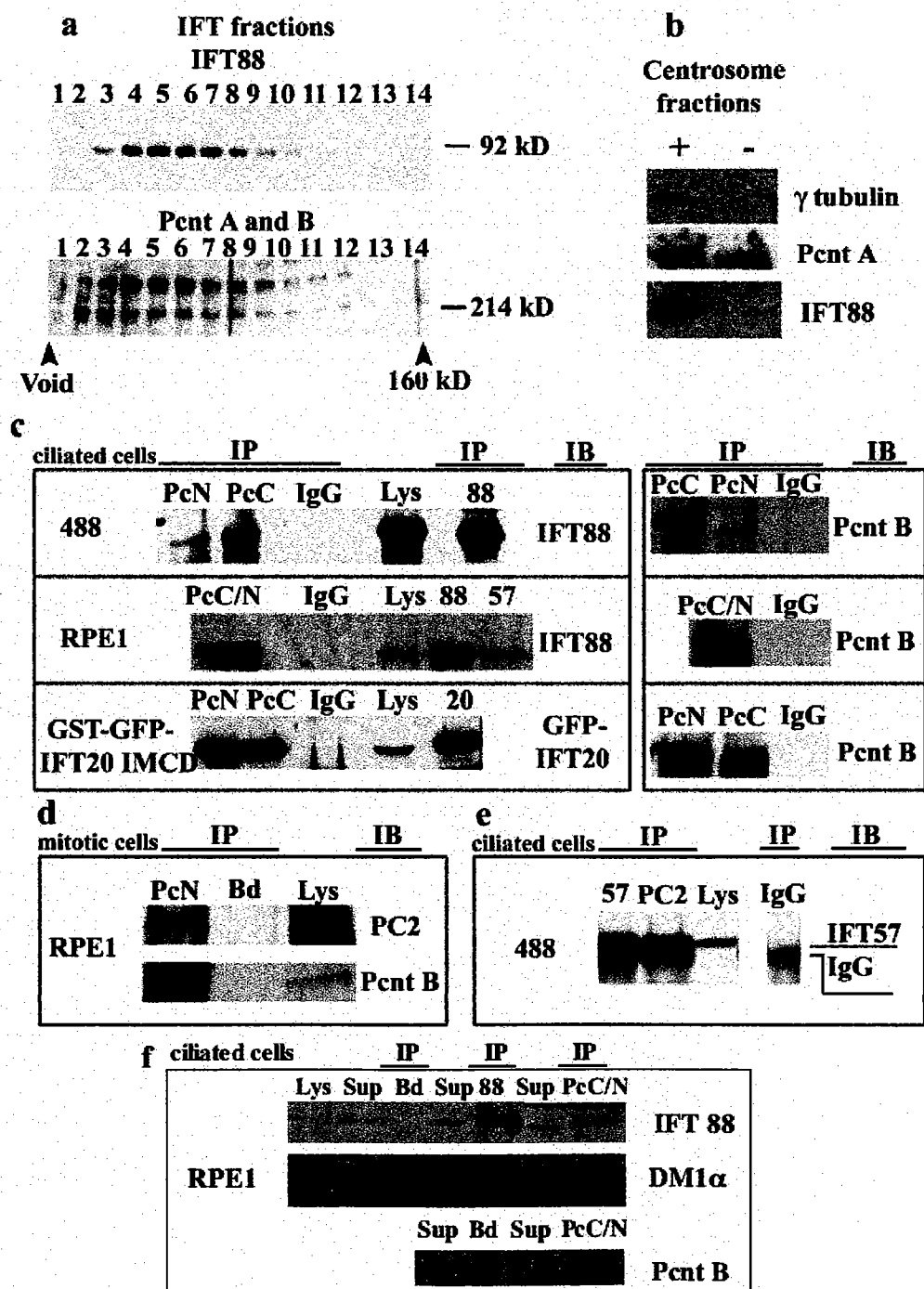


Figure 6. Pcnt interacts with proteins involved in cilia assembly and function. (a) Pooled IFT fractions from a sucrose gradient from mouse testes were applied to an FPLC Column and fractions were loaded on SDS gels and probed with Pcnt antibodies or IFT88 antibody. (b) Pooled peak centrosome fractions from sucrose gradients (+) containing γ tubulin, Pcnt and IFT88 as indicated and pooled noncentrosome fractions (-). (c, upper panel) Pcnt N- and C-terminal antibodies (PcN, PcC) independently immunoprecipitated endogenous IFT88 from lysates of ciliated 488 cells. IgG, nonimmune rabbit IgG, lysates (Lys) showing IFT88 at right. Pcnt immunoprecipitation confirmed, right. (c, middle panel) PcN/C immunoprecipitated IFT88 from ciliated RPE1 cells, as did antibodies to IFT88 and IFT57 but not rabbit IgG. (c, bottom panel) PcN and PcC pull down a GST-GFP-IFT20 fusion protein from a cell line stably overexpressing the protein, as does a glutathione column (IFT20), but not nonimmune IgG. Blots were probed with anti-GFP antibodies, immunoprecipitation with Pcnt (right panel), IB, immunoblot antibody. (d) PcN immunoprecipitated PC2 from mitotic RPE1 cells while beads alone do not (Bds). Pcnt immunoprecipitation confirmed by immunoblot (Pcnt B). (e) PC2 antibody, but not Rabbit IgG, immunoprecipitated IFT57 from ciliated 488 cells. IFT57, upper band. Lower band, antibody heavy chain. (f) PcC/N immunoprecipitated endogenous IFT88 from lysated of ciliated RPE1 cells and not α -tubulin. Lysate (Lys) indicate the starting material, supernatants of the immunoprecipitations are shown to the left of each immunoprecipitations. A half of the immunoprecipitations were loaded and 3% of immunoprecipitations are shown in the supernatants and lysates with an exception in d. in figure 6 d all the immunoprecipitations were loaded and 7% of immunoprecipitations are shown in the lysates. Jovanal San Agustin contributed figure 6 a, Keith Mikule provided centrosome fractions for figure 6 b, and Adam Gromley contributed figure 6 d and Agata Jurczyk contributed figures 6 b-c, e, and f.

FIGURE 6



Chapter II

**A Novel Human Protein of the Maternal Centriole is
required for the Final Stages of Cytokinesis and Entry
into S phase**

Abstract

Centrosomes nucleate microtubules and contribute to mitotic spindle organization and function. They also participate in cytokinesis and cell cycle progression in ways that are poorly understood. Here we describe a novel human protein called centriolin that localizes to the maternal centriole and functions in both cytokinesis and cell cycle progression. Centriolin silencing induces cytokinesis failure by a novel mechanism whereby cells remain interconnected by long intercellular bridges. Most cells continue to cycle, reenter mitosis, and form multicellular syncytia. Some ultimately divide or undergo apoptosis specifically during the protracted period of cytokinesis. At later times, viable cells arrest in G1/G0. The cytokinesis activity is localized to a centriolin domain that shares homology with Nud1p and Cdc11p, budding and fission yeast proteins that anchor regulatory pathways involved in progression through the late stages of mitosis. The Nud1p-like domain of centriolin binds Bub2p, another component of the budding yeast pathway. We conclude that centriolin is required for a late stage of vertebrate cytokinesis, Perhaps the final cell cleavage event, and plays a role in progression into S phase.

Introduction

Centrosomes are the major microtubule-nucleating organelles in most vertebrate cells (Doxsey, 2001b). In mitosis, they contribute to spindle organization and function, and in interphase, they organize microtubule arrays that serve as tracks for transporting proteins, organelles, and chromosomes. The centrosome also anchors regulatory molecules and may serve as a central site that receives, integrates, and transmits signals that regulate fundamental cellular functions. The core of the centrosome is comprised of a pair of centrioles, microtubule barrels that appear to anchor microtubules (Chretien et al., 1997; Piel et al., 2000). Each centriole is surrounded by pericentriolar material or centrosome matrix, which nucleates the growth of new microtubules and seems to be organized by the centrioles (Bobinnec et al., 1998). Although best known for their role in microtubule nucleation, recent data suggest that centrosomes also play key roles in cytokinesis and cell cycle progression.

A role for centrosomes in defining the site of cell cleavage during cytokinesis has been suggested for some time (Rappaport, 1986). Recent studies with vertebrate cells provide evidence for a direct link between centrosome activity and completion of cytokinesis.

Elimination of centrosomes from interphase cells by removal with a microneedle (Hinchcliffe et al., 2001) or from mitotic cells by laser ablation (Khodjakov and Rieder, 2001) caused cytokinesis defects, arrest, or failure. In another study, it was shown that during the final stages of cytokinesis, the maternal centriole moved to the intercellular bridge, the microtubule-filled interconnection between nascent daughter cells (Piel et al.,

2001). Centriole repositioning correlated with bridge narrowing and microtubule depolymerization, while movement of the centriole away from the bridge correlated with cell cleavage or abscission. The authors suggested that the maternal centriole might anchor a regulatory pathway that controls the final stages of cell division in vertebrate cells. This would be analogous to regulatory pathways anchored at spindle pole bodies (the centrosome equivalent) in budding and fission yeasts that control mitotic exit and cytokinesis (for reviews see (Bardin and Amon, 2001; McCollum and Gould, 2001; Pereira and Schiebel, 2001). However, no vertebrate pathway analogous to the mitotic exit network (MEN)* in budding yeast or septation initiation network (SIN) in fission yeast has been identified (Glotzer, 2001; Guertin et al., 2002). Moreover, the role of centrosome-associated molecules in the process of cytokinesis is poorly understood.

In addition to their role in cytokinesis, centrosomes appear to have a role in cell cycle progression. Recent evidence demonstrates that vertebrate cells lacking centrosomes do not initiate DNA replication (Hinchcliffe et al., 2001; Khodjakov and Rieder, 2001). The authors suggested that centrosomes controlled entry into S phase by recruiting or concentrating “core” centrosome molecules required for this process or that they indirectly activated a cellular checkpoint that monitored aberrant centrosome number. In another experimental system, vertebrate cells treated with cytochalasin D to inhibit actin-mediated cell cleavage also arrested cells in G1 as binucleate cells with supernumerary centrosomes (Andreassen et al., 2001). Although these results suggest that changes in centrosome number can affect entry into S phase, the precise role of centrosomes in cell

cycle progression in vertebrate cells will require identification of the molecular components and pathways that control these events.

In this paper, we identify a novel component of the vertebrate maternal centriole called centriolin. Abrogation of centriolin function by small interfering RNA (siRNA) silencing, overexpression, or antibody inhibition produces cytokinesis failure and G1/G0 arrest, just as seen when centrosomes are experimentally eliminated from cells. Centriolin silencing produces a novel cytokinesis phenotype in which dividing cells remain interconnected by long strands of cytoplasm and fail to cleave. The cytokinesis activity lies in a centriolin domain that is homologous to the MEN/SIN components Nud1p/Cdc11p and binds the Nud1p-interacting GTPase activating protein Bub2p. We conclude that centriolin is required for a distinct step in the final stages of vertebrate cytokinesis and can influence entry into S phase.

Results

Identification and cloning of a novel protein localized to the maternal centriole and intercellular bridge

Using sera from patients with the autoimmune disease scleroderma that react with centrosomes (Doxsey et al., 1994), we screened a human placenta gt11 cDNA expression library to identify genes encoding the autoantigens. Of the 3106 clones screened, only one of 1.7 kb was identified, indicating that the mRNA for this molecule was rare. The full-length cDNA was obtained, and the protein encoded by the cDNA was called

centriolin (see below and Materials and methods). The amino acid sequence of centriolin predicted a protein with several coiled-coil regions interrupted by noncoiled domains (Lupas, 1991) (Fig. 7 a). Two domains within the centriolin sequence shared homology with human oncogenic transforming acidic coiled-coil proteins (TACCs), which localize to centrosomes and are implicated in microtubule stabilization and spindle function (Lee et al., 2001). Another domain of centriolin was homologous to human stathmin, an oncogenic protein involved in microtubule destabilization (Andersen, 2000). The carboxy terminus of centriolin was identical to CEP110, a naturally occurring fusion to the fibroblast growth factor receptor that localizes to centrosomes, is oncogenic, and is of unknown function (Guasch et al., 2000). The relationship of CEP110 to centriolin is unknown, although we did not identify a cDNA corresponding to this protein in our library screens. A region of centriolin near the amino terminus shared homology with Nud1p and Cdc11p, budding and fission yeast spindle pole body proteins that anchor components of the yeast MEN and SIN, respectively, and are required for completion of mitosis and cytokinesis (Bardin and Amon, 2001; McCollum and Gould, 2001; Pereira and Schiebel, 2001; Guertin et al., 2002). The 120-amino acid region of shared homology between the Nud1 domain, Nud1p, and Cdc11p all have leucine-rich repeats and are predicted to form β helix structures in tertiary structure prediction programs. Antibodies raised against recombinant centriolin recognized a band of ~270 kD on Western blots of isolated centrosome fractions, whereas preimmune sera showed no specific bands (Fig. 7 b, Centrosome fractions). In vitro translation and overexpression of the protein in mammalian cells using the full-length cDNA produced a protein with a molecular weight

similar to the endogenous protein (Fig. 7 b, In vitro translated and Overexpressed) and to a protein predicted from the cDNA sequence (see Materials and methods).

Immunofluorescence microscopy demonstrated that centriolin was localized to centrosomes in a wide variety of species, including human, monkey, hamster, mouse, and *Xenopus* (Figs. 7 and 8). Centrosome localization was confirmed by showing that an HA-tagged centriolin protein ectopically expressed in COS cells localized to centrosomes (Fig. 8 a). The endogenous protein was present on the centrosome throughout the cell cycle. In late G1/early S phase, centrosomes begin to duplicate, and by G2/M, duplication is usually completed. During the duplication process, centriolin was present on only one of the two duplicating centrosomes, although other proteins, such as γ -tubulin, were found on both (Fig. 7 c, G2 cell). Beginning at late G2/prometaphase, dim staining was observed next to a brightly stained centrosome. By metaphase, when centrosomes become "mature," both centrosomes had equally high levels of centriolin and were more brightly stained than at any other cell cycle stage. This demonstrates that centriolin is a marker for centrosome maturation, a characteristic shared with cenexin (Lange and Gull, 1995) and ninein (Mogensen et al., 2000). At the metaphase to anaphase transition, centriolin staining diminished at centrosomes and reached its lowest levels by late anaphase/telophase. During cytokinesis, centriolin sometimes appeared as one or two dots adjacent to the intercellular bridge, suggesting that the centrosome/centriole had moved to this site (Fig. 7 c, Telo early). This staining pattern was consistent with recent time-lapse imaging experiments showing that the maternal centriole translocates to the intercellular bridge during cytokinesis (Piel et al., 2001). Centriolin next appeared as

diffusely organized material within the intercellular bridge and ultimately became concentrated at the midbody (Fig. 7 c, Telo late). The organization of centriolin at the centrosome was more precisely determined by serum starving cells to induce growth of a primary cilium from the maternal centriole (Vorobjev and Chentsov, 1982). In these cells, centriolin staining was confined to the maternal centriole underlying the cilium (Fig. 8 b). Immunogold electron microscopy on centrosome fractions (Doxsey et al., 1994; Blomberg and Doxsey, 1998) confirmed localization to the maternal centriole (Fig. 8 e, M) and further demonstrated that the protein was concentrated on subdistal appendages, specialized substructures of the maternal centriole implicated in microtubule anchoring (Fig. 8, c–e) (Chretien et al., 1997; Piel et al., 2000). Based on its centriolar localization, the protein was named centriolin. Centriolin was also found at noncentrosomal apical bands of material in specialized epithelial cells that lack proteins involved in microtubule nucleation and appear to anchor the minus ends of microtubules (Mogensen et al., 1997) (Fig. 8, f and g).

Centriolin silencing by siRNA induces cytokinesis failure and a novel cytokinesis phenotype

To determine the function of centriolin, we reduced its levels using siRNAs (Fire et al., 1998; Elbashir et al., 2001). Treatment of telomerase-immortalized diploid human retinal pigment epithelial (RPE-1) cells (Morales et al., 1999) with centriolin-specific siRNAs caused a significant reduction in centriolin mRNA levels (Fig. 9 a). Although we were unable to examine protein levels by Western blotting of whole cell lysates due to the rare

nature of this and other centrosome autoantigens (Doxsey et al., 1994), immunofluorescence staining demonstrated that centriolin was undetectable, or greatly reduced, at centrosomes in most cells (86%; $n = 1,012$). Quantitative analysis showed that immunofluorescence signals at individual centrosomes were significantly below those in cells treated with control lamin A/C siRNA, despite severe disruption of the nuclear lamina in the latter (Fig. 9 b) (Elbashiret et al., 2001). Midbody staining of centriolin was also reduced in cells treated with siRNAs targeting centriolin. Because centriolin shares homology with proteins known to affect microtubule organization and cytokinesis, we examined cells with reduced centriolin for defects in these functions. The most obvious cellular change detected in RPE-1 cells with reduced centriolin was a dramatic increase in the percentage of late-stage mitotic cells (~70-fold increase; Fig. 9 c). In addition, we observed an increase in the percentage of binucleate cells in three different cell lines, suggesting that a certain proportion of cells failed to cleave (Fig. 9 d; see below). The incidence of binucleate cells was significantly greater than controls, although somewhat lower than that observed for some other proteins involved in cytokinesis (Matuliene and Kuriyama, 2002; Meraldi et al., 2002; Mollinari et al., 2002). A similar cytokinesis phenotype was observed with a second set of siRNAs targeting a different centriolin sequence and with morpholino antisense DNA oligonucleotides targeting centriolin. The dramatically high percentage of cells in late mitotic stages suggested a unique cytokinesis defect in these cells. When carefully analyzed by immunofluorescence microscopy, cells with reduced centriolin appeared to be arrested or delayed in the final stages of cytokinesis. Most cells retained intercellular bridges of varying length and thickness (Fig.

9, m and n, arrowheads). In some cases, cells remained connected even though one or both of the future daughter cells had reentered mitosis (Fig. 9 n, M). Some cells failed to cleave, forming syncytia with two, three, or four cells remaining interconnected (Fig. 9, m and n). During the early stages of cytokinesis, midbodies appeared normal. A more complete understanding of the mechanism of cytokinesis failure was obtained by imaging live HeLa cells treated with centriolin-specific siRNAs (Fig. 10; see Videos 1–3, available at <http://www.jcb.org/cgi/content/full/jcb.200301105/DC1>). As expected, control cells (lamin siRNA) performed a distinct cell cleavage event with normal timing (average 2 h after mitosis) and immediately flattened and crawled apart (Fig. 10 a). Cells silenced for centriolin progressed normally through mitosis (Fig. 9, g–j; Fig. 10 e) and sometimes cleaved normally, but most failed to cleave or cleaved after prolonged periods of time (up to 23.2 h after metaphase; Fig. 10, b–d and f). These cells arrested or delayed in a unique post-telophase state. Most were unusually elongated, each with a persistent intercellular bridge of variable diameter that was often dynamic. Bridges alternated between thin threads of interconnecting cytoplasm to very thick interconnections of large diameter that appeared able to produce membrane ruffles (Fig. 10 b, 5:50, arrow). Midbodies were not detected within persistent interconnections between cells, suggesting that they were lost sometime during the protracted period spent in cytokinesis. Interconnected cells sometimes coalesced to form single cells and then quickly moved apart again (Fig. 10 d). They sometimes made multiple failed attempts at cleavage, but in no case did we observe a cell that formed a stable binucleate. This suggested that binucleate cells observed in fixed cells (Fig. 9 d) were transient intermediates in a process

that involved multiple failed attempts at cytokinesis. Cells that retained intercellular connections for long periods of time continued to progress through the cell cycle. To our surprise, some cells reentered the next mitosis while still interconnected and produced interconnected “progeny” that formed two- to four-cell syncytia, thus confirming the cell–cell interconnections observed by indirect immunofluorescence (Fig. 9, m and n). In some cases, cells that remained interconnected for long periods of time appeared to undergo apoptosis. They showed extensive blebbing, increased phase density, and decreased size and lifted from the substrate (Fig. 10 b, upper cell, 7:20). Microtubule organization in cells with reduced centriolin appeared normal at all cell cycle stages. This included microtubules of the spindle midzone in anaphase and the midbody in telophase (Fig. 9, e–j). Microtubule nucleation from centrosomes also appeared normal (Fig. 9, k and l), although a slight delay in recovery was sometimes observed within the first minute or two. γ -Tubulin, a marker for centrosome-associated microtubule nucleation, was localized normally to centrosomes (Fig. 9 b), as were several other centrosome antigens, including GCP-2 (Murphy et al., 1998) and cNap-1 (Fry et al., 1998). Midbody markers, such as anillin (see Glotzer, 2001) and γ -tubulin (Shu et al., 1995), were also localized normally. At later stages of cytokinesis in cells with long intercellular bridges, midbodies were no longer detected. These data indicate that cytokinesis failure did not result from disruption of microtubules, centrosomes, or midbodies.

Overexpression of centriolin and its Nud1 domain induces cytokinesis failure in a microtubule-independent manner

We next tested the effect of ectopic expression of centriolin and its Nud1 domain on cytokinesis and microtubule organization (Fig. 11, a–g). The most striking defects in COS-7 cells expressing HA-tagged centriolin were an increase in the proportion of telophase cells and the formation of binucleate cells (Fig. 11 g). Microtubule bundles were observed within intercellular bridges in telophase cells (Fig. 11 a), but they did not appear to cause binucleate cell formation. We found that overexpression of the 120–amino acid GFP-tagged Nud1 domain of centriolin was sufficient to induce cytokinesis failure and binucleate formation (Fig. 11, e and g) in the absence of detectable changes in microtubule organization (Fig. 11, c and d) and without disrupting endogenous centriolin from centrosomes (Fig. 11 f). The results from gene silencing and protein overexpression support a microtubule-independent mechanism for cytokinesis failure.

The centriolin Nud1 domain interacts with the yeast Bub2p in vitro

Budding yeast Nud1p anchors the MEN to the spindle pole body through direct interactions with Bub2p and perhaps other MEN components (Gruneberg et al., 2000); (Pereira et al., 2000). To determine if the centriolin Nud1 homology domain (Fig. 11 h) had similar properties, we tested its ability to bind Bub2p by directed two-hybrid analysis and immunoprecipitation. Because no vertebrate Bub2p homologue has been unequivocally identified (Cuif et al., 1999), we examined the ability of the centriolin Nud1 domain to interact with yeast Bub2p. Both two-hybrid analysis and

immunoprecipitation from yeast cells coexpressing the two proteins revealed a strong and specific interaction between the centriolin Nud1 domain and Bub2p (Fig. 11, i and j). No signal was observed when either protein was used alone, and no binding was detected between the centriolin Nud1 domain and the budding yeast MEN component Bfa1p, consistent with interaction observations in budding yeast (Pereira and Schiebel, 2001).

Cleavage failure is observed in *Xenopus* embryos injected with centriolin antibodies

A third approach was used to examine centriolin function. When affinity-purified anticentriolin antibodies (Fig. 7 b) were microinjected into one cell of two-cell *Xenopus* embryos (Doxsey et al., 1994), the injected cell failed to cleave, or cleaved a few times and then arrested; uninjected cells or preimmune IgG-injected cells divided normally (Fig. 12, a and d). Centriolin antibody-injected cells arrested with two nuclei and two well-organized microtubule asters, indicating that karyokinesis and microtubule organization were normal, but cells failed to complete the final event of mitosis, cell cleavage (Fig. 12 c). Preimmune IgG-injected cells had a single nucleus with one or two microtubule asters, depending on their cell cycle stage, as would be expected for cells that had undergone normal cell cleavage (Fig. 12 b). Taken together, the results from gene silencing, antibody injection, and protein overexpression in several experimental systems all demonstrate that centriolin plays an important role in the late stages of cytokinesis.

siRNA-induced gene silencing of centriolin causes G1/G0 arrest

Cytokinesis defects and delays induced by centriolin silencing were observed at early times after treatment of RPE-1 cells (18–24 h). At later times (48–72 h after treatment), a reduction in the mitotic index was observed, suggesting that the cells were arrested at some other stage of the cell cycle. This was directly tested by treating cells with nocodazole to induce mitotic arrest and quantifying mitotic cells in DAPI stained preparations. Under these conditions, most lamin siRNA-treated control RPE-1 cells were arrested in mitosis (71%), whereas only a small fraction of centriolin siRNA-treated cells arrested at this cell cycle stage (<1%). To determine the cell cycle stage of arrest, cells were analyzed by flow cytometry. In the presence of nocodazole, control cells showed a significant shift from the G1 peak to the G2/M peak (Fig. 13 a, red). In contrast, cells treated with siRNAs targeting centriolin did not significantly shift into the G2/M peak in the presence of nocodazole but remained largely in G1 (Fig. 13 a, blue). The inability to undergo a nocodazole induced shift into the G2/M peak was a feature shared by cells driven into G0 by serum starvation (Fig. 13 b, blue). The proportion of cells in S phase was either unaltered or slightly decreased in cells silenced for centriolin both in the presence of nocodazole (centriolin, 13%; lamin, 23%) or in its absence (centriolin, 13%; lamin, 19%). These results demonstrate that cells with reduced centriolin arrest before S phase, possibly in G1/S, G1, or G0. Ki-67 staining was also used to examine the stage of cell cycle arrest. Ki-67 is an antibody directed against a nuclear protein that stains cycling cells or cells arrested in cycle (e.g., G1/S or S phase; (Gerdes et al., 1984)) but not cells that are quiescent (G0) or differentiated. As expected,

nearly all untreated RPE-1 cells or control cells treated with siRNAs targeting GFP or lamins A/C were positive for Ki-67 (Fig. 13, c and d). However, most cells with reduced centriolin had undetectable levels of Ki-67 staining (Fig. 13, c and d). Taken together, results from mitotic index assays, flow cytometry, and Ki-76 staining in RPE-1 demonstrated that reduction of centriolin levels prevented cells from entering S phase and appeared to drive them out of cycle into a G0-like state. This cell cycle arrest effectively prevents the initiation of additional rounds of centrosome duplication in cells compromised by having diminished levels of centriolin.

Discussion

In this paper, we characterize centriolin, a maternal centriole component whose disruption induces cytokinesis failure and G1/G0 arrest. The ability of centriolin to induce this phenotype may provide a molecular explanation for the cytokinesis defects and G1 arrest previously observed in vertebrate cells after experimental removal of entire centrosomes (Hinchcliffe et al., 2001; Khodjakov and Rieder, 2001). Moreover, association of centriolin with the maternal centriole may be a molecular requirement for activation and completion of the final stages of cytokinesis, functions recently suggested for the maternal centriole in vertebrate cells (Piel et al., 2001). The cytokinesis phenotype observed in cells treated with siRNAs targeting centriolin is uncommon among proteins that function in cytokinesis. The predominant phenotype observed after functional abrogation of most proteins that cause cytokinesis failure is coalescence of dividing cells into a single cell with two nuclei. This has been shown for proteins of the central spindle,

regulatory proteins that control cytokinesis, microtubule-associated proteins, and the centrosome proteins γ -tubulin and centrin (Shu et al., 1995; Kaiser et al., 2002; Manabe et al., 2002; Matuliene and Kuriyama, 2002; Meraldi et al., 2002; Mollinari et al., 2002; Salisbury et al., 2002; Seong et al., 2002). In contrast, the predominant cytokinesis phenotype observed in cells with reduced centriolin is failure to resolve persistent intercellular bridges between dividing cells. The apparent consequences of this event are generation of multicellular syncytia, continuous attempts at cell cleavage that include binucleate cells as intermediates, completion of cytokinesis, perhaps artificially, by traction-mediated cytokinesis (Burton and Taylor, 1997), and apoptotic cell death. Although we have not determined the precise mechanism of cytokinesis failure in cells with abrogated centriolin function, we are testing whether membrane is incorporated normally into the cleavage site (Finger and White, 2002; Thompson et al., 2002). Persistent intercellular bridges have also been observed between dividing vertebrate cells overexpressing the Cdc-14A phosphatase (Kaiser et al., 2002). This uncommon phenotype has thus far been observed only with proteins (centriolin and Cdc14A) that share homology with components of yeast regulatory pathways that control mitotic exit and cytokinesis (MEN/SIN) and localize to the same intracellular sites as the yeast proteins (centrosome/spindle pole bodies). Persistent intercellular connections may also be present in cells lacking centrosomes and may reflect a similar type of cytokinesis defect (Doxsey, 2001a). Although the mechanism of cytokinesis failure appears to be different in SIN mutants, the outcome is the same, production of bi and multinucleate cells. These observations support the idea that vertebrate cells may possess regulatory

pathways that function in much the same way as those in yeast to coordinate the final stages of cytokinesis with chromosome segregation. Several domains of centriolin share sequence homology with proteins implicated in tumorigenesis, including the TACCs and oncoprotein 18/stathmin. In this paper, we show that the domain homologous to Nud1p/Cdc11p can induce aneuploidy through cytokinesis failure. This event could generate further genetic instability through the organization of multipolar spindles by supernumerary centrosomes and could thus facilitate the accumulation of activated oncogenes and loss of tumor suppressor genes (Pihan et al., 2001; Doxsey, 2002). We are currently investigating the role of centriolin in human oncogenesis. Our results suggest that minor changes in centrosome composition, such as loss of centriolin, can arrest cells in G1/G0. Because cells with reduced centriolin have difficulty completing the final stages of cytokinesis, it is tempting to suggest that G1/G0 arrest is a consequence of improper cytokinesis. However, it has been suggested that G1 arrest in cells lacking centrosomes may also result from the loss of core centrosome components, improper spindle alignment, or the presence of excess DNA in binucleate cells (Andreassen et al., 2001; Hinchcliffe et al., 2001; Khodjakov and Rieder, 2001; Meraldi et al., 2002). We are currently testing a model in which the loss of core centrosome components activates a checkpoint involved in monitoring "centrosome integrity" and thus prevents centrosome duplication by arresting cells in G1/G0, as we and others have proposed (Doxsey, 2001a; Quintyne and Schroer, 2002).

Materials and methods

Cell culture and transfections

The cells used primarily in this study were diploid, telomerase-immortalized human RPE-1 cells (hTERT-RPE-1s; CLONTECH Laboratories, Inc.) (Morales et al., 1999). Other cells included HeLa, COS-7, hTERT-HME-1 (human mammary epithelia), U2OS, and *Xenopus* tissue culture (XTC) cells. All were grown as previously described (American Type Culture Collection). COS-7 cells were transfected as previously described (Lipofectamine; Invitrogen).

Antibodies

Amino acids 268-903 of centriolin were fused with GST (CLONTECH Laboratories, Inc.), overexpressed in *Escherichia coli*, and purified as previously described (Doxsey et al., 1994). Antibodies raised in rabbits were affinity purified by passing sera over a GST column to remove anti-GST antibodies and then over a SDT-centriolin column.

Antibodies to the following proteins were also used in this study: lamin A/C (Cell Signaling Technology), α - and γ -tubulins (Sigma-Aldrich), LexA (Santa Cruz Biotechnology, Inc.), GAL4 transactivation domain (TAD) (CLONTECH Laboratories, Inc.), Ki-67, and HA (BD Biosciences).

Immunofluorescence and electron microscopy

Cells were prepared for immunofluorescence, imaged, and deconvolved (Metamorph; Universal Imaging Corp.), and centrosomes were quantified as previously described

(Dictenberg et al., 1998). All immunofluorescence images are two-dimensional projections of three-dimensional reconstructions to ensure that all stained material was visible in two-dimensional images. Immunogold electron microscopy was performed as previously described (Doxsey et al., 1994) using centrosome fractions from HeLa cells (Blomberg and Doxsey, 1998) and antibodies to centriolin followed by antibodies coupled to 5-nm gold particles (Amersham Biosciences). Pillar cells were prepared and stained as previously described (Mogensen et al., 1997).

Centriolin cloning

A cDNA of ~1.7 kb was identified by screening a human placenta expression library with serum from individuals with scleroderma (Doxsey et al., 1994). The nucleotide sequence was compared with others (blastn) in the human genome database (National Center for Biotechnology Information) and revealed a sequence with 99% identity on chromosome 9 q34.11-34.13. Genscan predicted an ~7-kb gene comprising 40 exons. PCR primers were used to obtain an ~7-kb cDNA in a human testes cDNA library. The 5' end, obtained by rapid amplification of cDNA ends (RACE), was identical to the predicted sequence. A full-length HA-tagged centriolin was obtained by inserting an HA tag (YPYDVPDYASL) 5' to the RACE fragment and ligating the HA-centriolin cDNA to the original fragment. The full length centriolin cDNA contained 6,975 nucleotides with an ORF of 2,325 amino acids and predicted a molecular mass of 269 kD, consistent with the molecular mass of endogenous centriolin (Fig.7).

Regions flanking the ORF had a translational start (Kozak sequence), polyadenylation sequence, poly-A tail, and multiple upstream and down-stream stop codons. The construct was inserted into pcDNA 3.1 Zeo (+) (Invitrogen) using BamHI and NotI restriction sites. Centriolin was translated in vitro (TNT; Promega) and expressed in cultured cells using conventional procedures (Lipofectamine). Centriolin amino acids 435-623 and 1385-1658 were 24% identical/47% similar and 20% identical/41% similar to the COOH-terminal half of TACCs, respectively. Amino acids 879-913 were 40% identical/51% similar to amino acids 72-106 of human stathmin. Amino acids 126-234 were 31-35% identical/47-50% similar to Nud1p and Cdc11p.

siRNA and morpholino antisense

siRNAs targeting centriolin, lamin A/C, and GFP mRNAs were made as complimentary single-stranded 19-mer siRNAs with 3' dTdT overhangs (Dharmacon Research), deprotected, annealed, and delivered into cells using a 400 μ M stock (Oligofectamine; Invitrogen). The nucleotides targeted were as follows: in centriolin, 117-136 and 145-163; in lamin A/C, 608-630; and in pEGFP-C1 (CLONTECH Laboratories, Inc.), 233-252. Fluorescein-conjugated morpholino antisense DNA oligonucleotides (Gene Tools) targeting the start codon of centriolin were introduced into cells using the EPE1 agent (Gene Tools). The inverse sequence was used as control.

Time-lapse imaging

HeLa cells plated on coverslips (25 mm diameter) were treated with siRNAs targeting centriolin for 50 h. They were placed in chamber (PDMI-2; Harvard Apparatus) in

complete medium with CO₂ exchange (0.5 liters/min) at 37°C . Cells were imaged every 10 min for 12-20 h using a 20x or 40x phase contrast lens with a green interference filter on an inverted microscope (Olympus IX-70). Images were captured on a CoolSnap HQ CCD camera (Roper Scientific) and concatenated using Metamorph software (Universal Imaging Corp.).

Primary cilium formation and microtubule nucleation

Primary cilia were induced by culturing hTERT-RPE-1 cells in medium with 0.25% serum for 48 h and identified using the GT335 antibody raised to polyglutamylated α - and β -tubulins (Bobinnec et al., 1998). Microtubule nucleation was performed as previously described (Purohit et al., 1999) by treatment with nocodazole (1 mg/ml) for 1 h at 37°C, fixing cells at various times after washing out drug, and then staining for microtubules.

RT-PCR

Centriolin mRNA levels were assayed by RT-PCR using 10 μ l mRNA (OneStep RT-PCR; QIAGEN; α -tubulin served as an internal control in the same reaction). All products were sequenced.

Yeast two-hybrid analysis and immunoprecipitations

A fragment containing amino acids 127-233 of centriolin was cloned into EcoRI and Sall sites of pGADT7 (CLONTECH Laboratories, Inc.) to produce a fusion with the GAL4

TAD. Constructs pEG202 (LexA), pGP69 (LexA-*Bub2*), and pGP122 (LexA-*BFA1*) and the yeast strain SGY37 were from Elmar Schiebel (Peterson Institute for Cancer Research, Manchester UK). SGY37, which contains a *LacZ* reporter gene under the control of a LexA operator, was transformed with plasmid DNA using LiAc (Ito et al., 1983), and transformants were selected for on dropout medium. We used semiquantitative β -galactosidase assays with CPRG (chlorophenol red- β -D-galactopyranoside; Roche) as a substrate per the manufacturer's instructions. Coimmunoprecipitation of LexA and GAL4 TAD fusion proteins were performed as previously described (Schramm et al., 2001).

Flow cytometry

Cells treated with siRNA for 50-70 h were treated with 100 ng/ml for 12 h, removed from plates, and fixed in methanol. Cells stained with propidium iodide were analyzed by flow cytometry (FACSCAN; Becton Dickinson) using Flojo software (Tree Star, Inc.).

GeneBank/EMBL/DDBJ accession numbers

The GenBank/EMBL/DDBJ accession number for centriolin is AF513978 and for lamin A/C is X03444.

Online supplemental material

Supplemental videos (Videos 1-3) are available at

<http://www.jcb.org/cgi/content/full/jcb.200301105/DC1>. The supplemental videos show

that cells silenced for centriolin delay in cytokinesis, remain interconnected by persistent intercellular bridges, re-enter mitosis while still interconnected, and form multicellular syncytia. Some cells divide normally while others undergo apparent apoptosis characterized by blebbing, rounding up, diminution in size, and loss of substrate attachment.

Figure 7. Centriolin is a ~270-kDa coiled-coil protein localized to mature centrosomes and the midbody. (a, top) Schematic showing centriolin domains that share homology with budding and fission yeast proteins Nud1p and Cdc11p, human stathmin, and human and *Drosophila* TACCs. Percentages represent identities and similarities of centriolin to the homologous proteins described above. (a, bottom) Schematic showing centriolin regions predicted to be coiled coil. Below both diagrams are centriolin amino acid numbers. (b, In vitro translated) [³⁵S]methionine-labeled HA-tagged centriolin produced by in vitro translation of cDNA and resolved directly (Cen) or after immunoprecipitation with HA antibodies (Cen IP); empty vector (Vec). (b, Overexpressed) Western blots probed with anti-HA antibody showing overexpressed HA-tagged centriolin (HA-Cen) and its absence from cells overexpressing β -galactosidase (β gal). (b, Centrosome fractions) Centrosome fractions prepared from HeLa cells and *Xenopus* tissue culture (XTC) cells blotted with antibodies to centriolin (Cen) or preimmune sera (PreI). Arrowheads show position of centriolin. In XTC cells, the bands below centriolin appear to be degradation products as they are sometimes observed in protein fractions produced by in vitro translation or overexpression. Bars represent positions of molecular weight markers ($\times 10^3$). (c) Immunofluorescence images of endogenous centriolin in RPE-1 cells at different cell cycle stages. The top panels show merged images of centriolin (green), γ -tubulin (red), and nuclei (blue) from cells in G1, G2, proM (premetaphase), M (metaphase), and anaphase (A). Insets, higher magnifications of centrosomes stained for γ -tubulin (left) and centriolin (right). Centriolin localization to one of the two centrosomes is demonstrated most clearly in the

G2 cell. Middle panels (Telo early) and bottom panels (Telo late) show separate images of γ -tubulin staining (left) and centriolin (right). γ -Tubulin marks both mother and daughter centrioles, which are separated in some cases. Centriolin staining is confined to one of two centrioles, which sometimes appears at the intercellular bridge (Telo early). Centrioles lacking centriolin are indicated by arrowheads in right panels. At later stages of telophase (Telo late), centriolin is also on the midbody. All immunofluorescence images (here and elsewhere) are two-dimensional projections of three-dimensional reconstructions to ensure that all stained material is visible. C, centriole; MB, midbody. Bar in c, 10 μ m. Centriolin sequencing was performed by Cytomix and Adam Gromley contributed the rest.

FIGURE 7

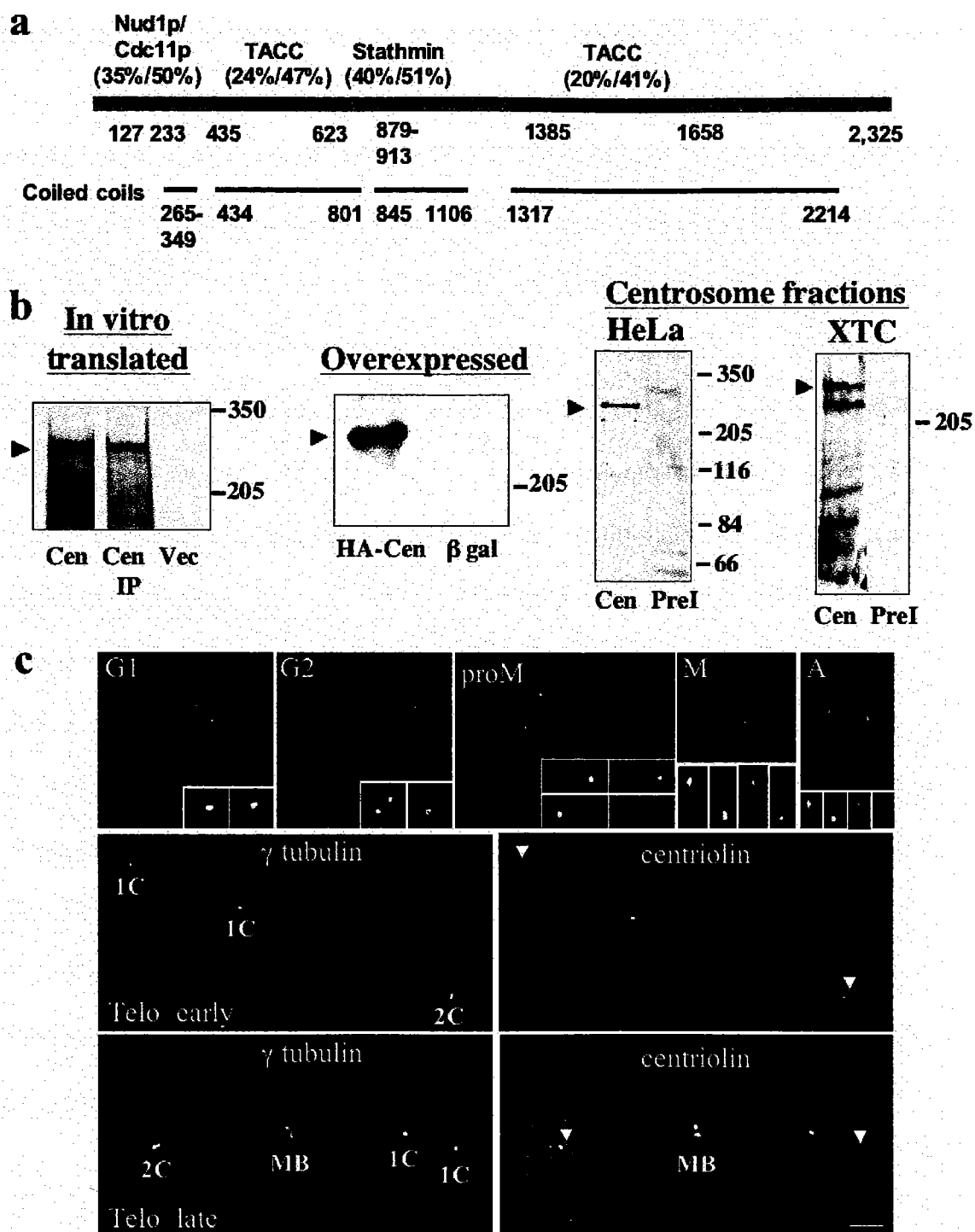


Figure 8. Centriolin is localized to maternal centrioles and noncentrosomal sites of microtubule anchoring. (a) HA-tagged centriolin overexpressed in COS-7 cells localizes to the centrosome (anti-HA, green) at the convergence of microtubules (red, anti- α -tubulin). (b) An RPE-1 cell immunostained with an antibody to polyglutamylated tubulin (GT335) (Bobinnec et al., 1998) to label centrioles and the primary cilium (red), and for centriolin (green), which is localized to the maternal centriole (m) associated with the primary cilium (yellow in merge) but not on the daughter centriole (d). n, nucleus. (c-e) Electron micrographs showing specific immunogold labeling of centriolin on subdistal appendages found on maternal (e, bottom, M) but not daughter centrioles (e, top, D). c and d are longitudinal and cross sections, respectively, through maternal centrioles, and e is a longitudinal section through both centrioles. Arrowheads show striations characteristic of subdistal appendages. (f and g) Centriolin is found at noncentrosomal sites of microtubule anchoring in pillar cells of the mouse cochlea (arrows) (Mogensen et al., 1997). (f) Schematic representation of pillar cell. (g) Centriolin immunofluorescence staining overlaid with phase contrast image. Centrosome and associated cilium are shown schematically at top of cell in f. Bars: (a and g) 10 μ m; (b) 2 μ m; (c-e) 100 nm.

Adam Gromley contributed figure 8 a, Agata Jurczyk contributed figure 8 b, Chris Powers and Maureen Blomberg contributed the electron microscope images, and Mette Mogensen contributed figure 8 f and g.

FIGURE 8

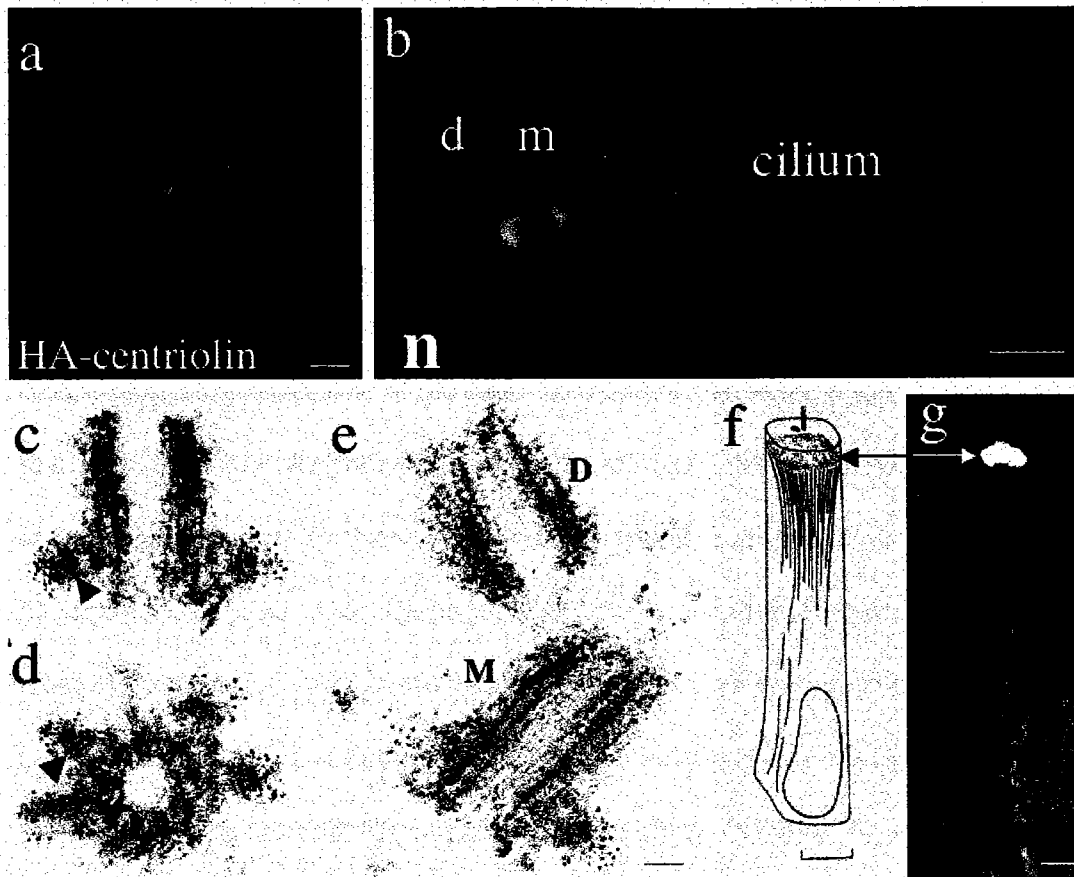


Figure 9. RPE-1 cells treated with siRNAs targeting centriolin retain persistent intercellular connections and fail in cytokinesis. (a) RT-PCR analysis shows that centriolin mRNA is reduced in RPE-1 cells treated with centriolin specific siRNAs (top right) but is unaffected in cells treated with siRNAs targeting lamin A/C (top left, sequence identity confirmed). Control (α -tubulin) RT-PCR was performed in the same reaction mixtures with centriolin and lamin (bottom panels). (b) Immunofluorescence images (top right; α -tubulin, red; centriolin, green) and quantification of centriolin levels in centrosomes from cells treated with siRNAs as indicated. The top right panes shows a cell with undetectable centriolin at the centrosome/centriole, and top left panel shows a cell that is unaffected by the treatment and stains for centriolin (green/white). Graph shows the average centriolin fluorescence intensity/pixel at individual centrosomes (bars) in cells treated with lamin or centriolin siRNAs. The centrosome fluorescence in most centriolin siRNA-treated cells (83%) was below the lowest values observed in control cells. (c) Graph showing a dramatic increase in the percentage of cells in telophase/cytokinesis after siRNA targeting of centriolin (~70-fold). N, total number of cells counted (c and d). (d) Graph showing the increased percentage of binucleate cells in HeLa, U2OS, and RPE-1 cell lines after treatment with centriolin siRNAs (4-15-fold greater than controls). In c and d, values represent data from single experiments representative of three to four experiments. The time analyzed was as follows: HeLa, 48 h and 72 h; U2OS, 72 h; RPE-1, 24 h. (e-l) Microtubule organization (e-j) and microtubule nucleation (k and l) are not detectably altered in cells treated with centriolin siRNA (f, h, j, and l) compared with cells treated with lamin siRNA (e, g, i, and k). Arrows indicate

position of centrosomes; no centrosome staining is observed in centriolin siRNA-treated cells. Insets in k and l are enlargements of centriolin staining at centrosomes (or microtubule convergence sites) at arrows. Cells in interphase (e and f, lower cell), prometaphase/metaphase (proM/M; g and h), and telophase (i and j) were labeled for microtubules (red), centrosomes (green/yellow), and nuclei (blue). MB, midbody. (m and n) Cells treated with siRNAs targeting centriolin were stained for microtubules (red) and DNA (blue). Arrowheads indicate contiguous connections between two or more cells. (m) Three interconnected cells form a syncytium. (n) One daughter of an interconnected pair of cells has reentered mitosis (M). Bar in n: (e-j) 5 μm ; (k,l, and insets) 3.5 μm ; (m and n) 15 μm . The siRNA for these experiments were done by Adam Gromley and Agata Jurczyk, all the counts and imaging were performed by Adam Gromley.

FIGURE 9

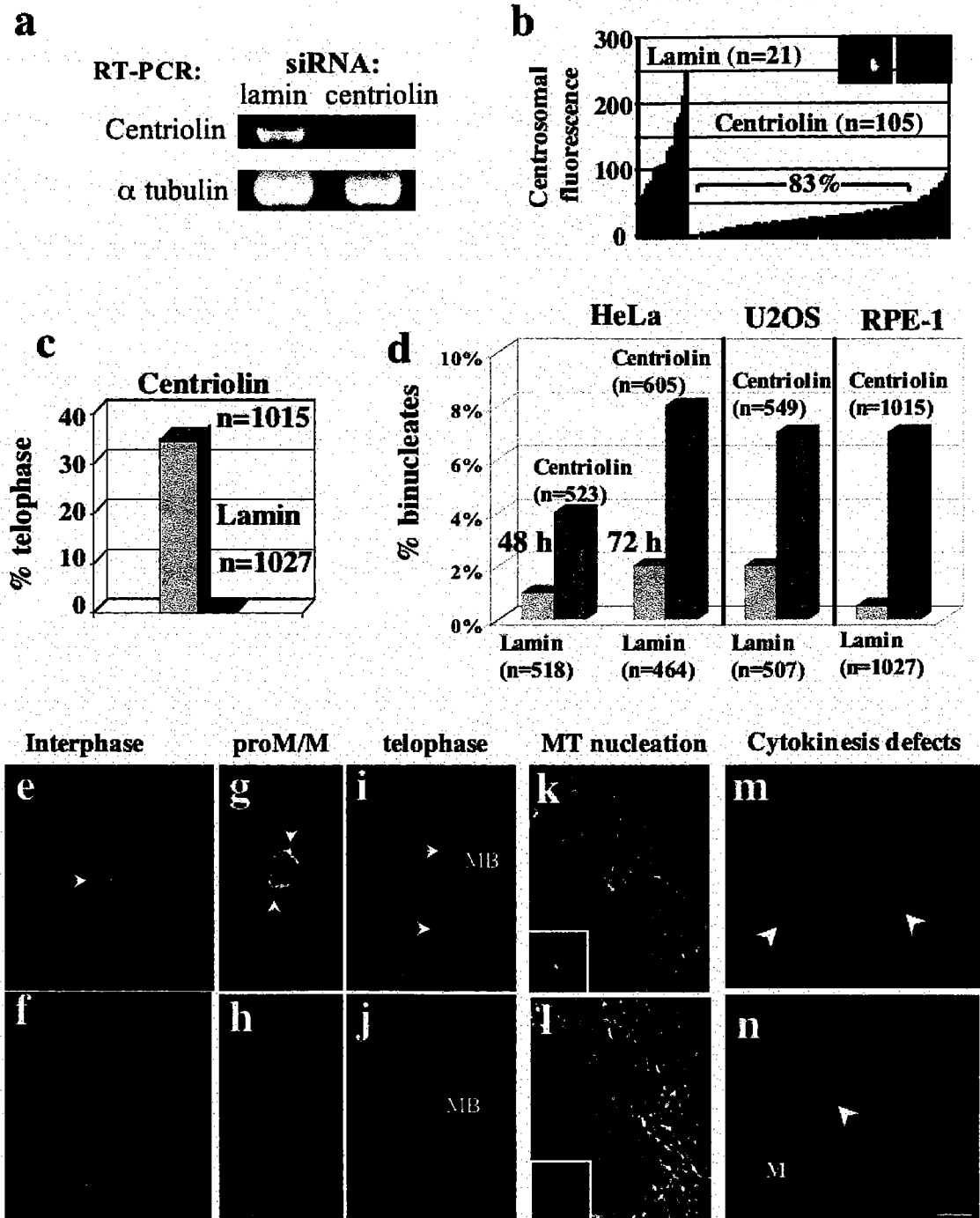


Figure 10. Time-lapse images of HeLa cells treated with centriolin siRNAs reveal unique cytokinesis defects. (a) A cell treated with control siRNAs targeting lamin moves apart, forms visible midbody (arrow), and completes the final cleavage event with normal timing (1-3 h after metaphase). (b-d) Centriolin siRNA-treated cells remain attached for extended periods of time through persistent intercellular bridges and sometimes do not show visible midbodies. (b) A cell that remains attached by a long intercellular bridge for at least 8 h. The cell cleaves, both daughter cells round up, and at least one appears to undergo apoptotic cell death (upper cell, 7:20, extensive blebbing and decrease in size). (c) A dividing cell that has not completed cleavage reenters the next mitosis. One cell rounds up and is drawn to the other. The other rounds up and both undergo the early stages of cytokinesis to form a total of four cells; these progeny often remain attached by intercellular bridges forming syncytia. (d) Cell showing three failed attempts at cell cleavage over a 9.5-h time period. (e) Cells treated with siRNAs targeting centriolin progress from nuclear envelope breakdown (NEB) to anaphase with normal timing, similar to lamin siRNA controls. Vertical bars represent recordings from single cells (e and f). (f) Centriolin siRNA-treated cells are delayed in cytokinesis (~70%) compared with control lamin siRNA-treated cells, a value consistent with a 70-80% silencing efficiency. Results represent recordings of individual cells from several independent experiments. Time in hours and minutes is included in each panel in a-d. Bar, 10 μ m. Timelapse videos (Videos 1-3) of the series of images shown in a-c are available at <http://www.jcb/cgi/content/full/jcb.200301105/DC1>. Agata Jurczyk contributed this figure.

FIGURE 10

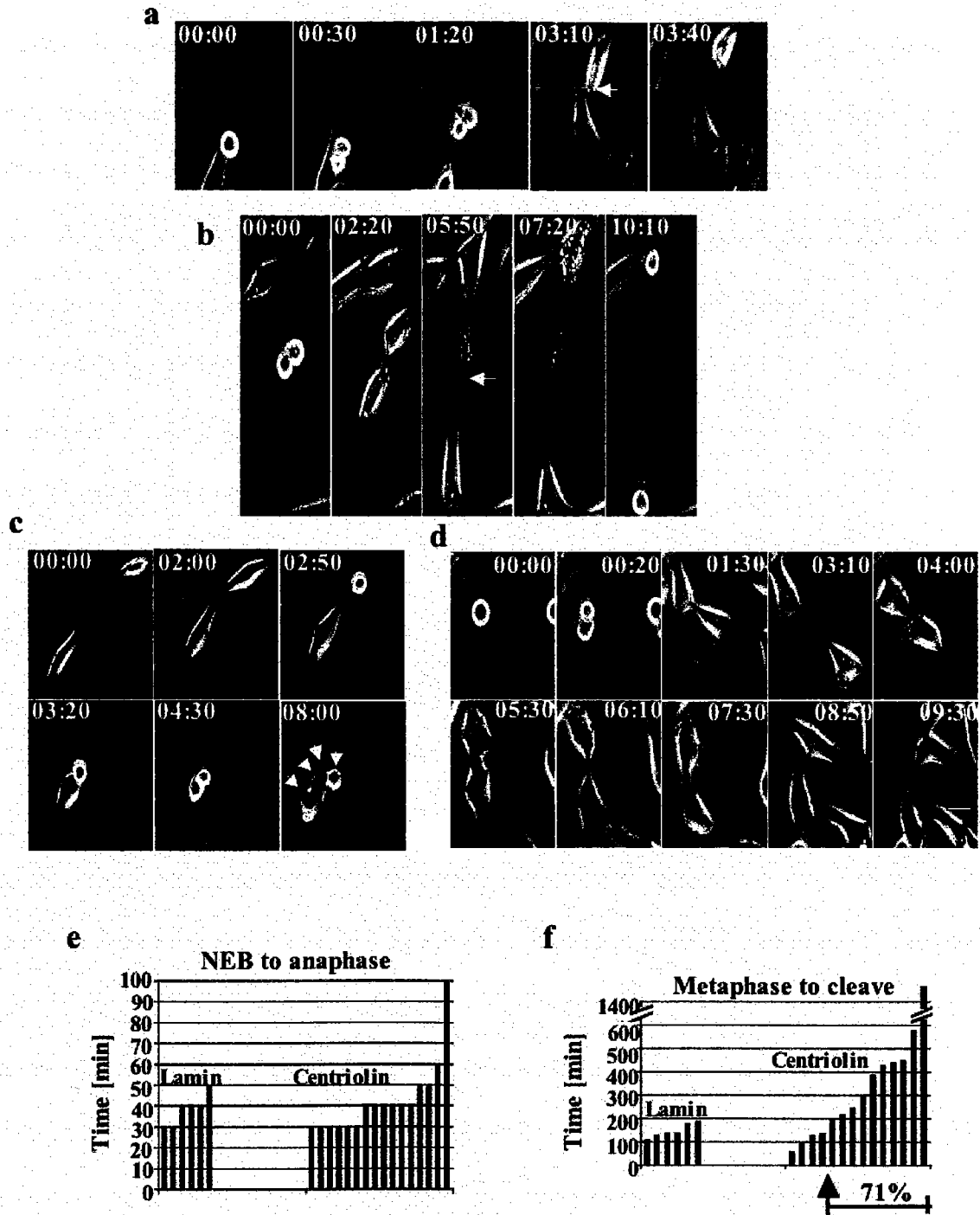


Figure 11. Cells expressing centriolin fail in cytokinesis, as do cells expressing the centriolin Nud1 domain that interacts with yeast Bub2p. (a) COS-7 cell

overexpressing HA-tagged centriolin (left inset) showing persistent microtubule bundles in the intercellular bridge during cytokinesis (main panel, α -tubulin staining) despite reformation of the nucleus and decondensation of chromatin (DNA, right inset). (b) Control COS-7 cell (expressing HA alone, bottom center) at a similar cell cycle stage based on nuclear morphology (bottom right) shows a narrow intercellular bridge and diminished microtubule polymer (center), characteristic of cells that have reformed nuclei and decondensed DNA. (c-f) COS-7 cells expressing a GFP-tagged Nud1 domain of centriolin (c and d, insets, green; DNA, blue) have normal intercellular bridges (d, telophase, arrowhead) and normal microtubule organization (c, interphase) as in controls. However, the cells (yellow) often become binucleate (blue) by a mechanism that does not involve disruption of the endogenous centrosome-associated centriolin (f; right inset shows enlargement of centrosome, left inset shows transfected cell). (g) Quantitative analysis showing that HA-centriolin and the GFP-tagged Nud1 domain both induce significant binucleate cell formation compared with controls (HA and GFP). Values are from a single experiment and are representative of three experiments. Bar, 7 μ m (for all panels). N, total number of cells counted. (h) Alignment of the centriolin Nud1 domain with the yeast Nud1p and Cdc11p proteins. (i) Direct yeast two-hybrid analysis demonstrates an interaction between the human Nud1 domain with one of the two components implicated in GTPase activating protein activity, Bub2p, but not Bfa1p. The blue colony in the blue box and increased β -galactosidase activity (bar 2 of graph)

demonstrate a specific interaction between the human centriolin Nud1 domain (hNud1) and yeast Bub2p. Bar 1, LexA-BUB2 x TAD; bar 2, Lex A-BUB x TAD-hNud1; bar 3, LexA-BFA1 xTAD; bar 4, TAD-hNud1 x LexA-BFA1; bar 5, TAD-hNud1 x LexA. (j) Specific coimmunoprecipitation of HA-tagged hNud1 and LexA-tagged yeast Bub2p from yeast cells. Coprecipitation was observed using antibodies to either protein and only when both were coexpressed (top middle panel in each group). Lane 1, TAD-HA-hNud1 x LexA; lane 2, TAD-HA-hNud1 x Bub2p-LexA; lane 3, TAD-HA x Bub2p-LexA. Adam Gromley contributed the figures a-h, James Silibourne contributed figure i, and Ensar Halilovic contributed figure j.

FIGURE 11

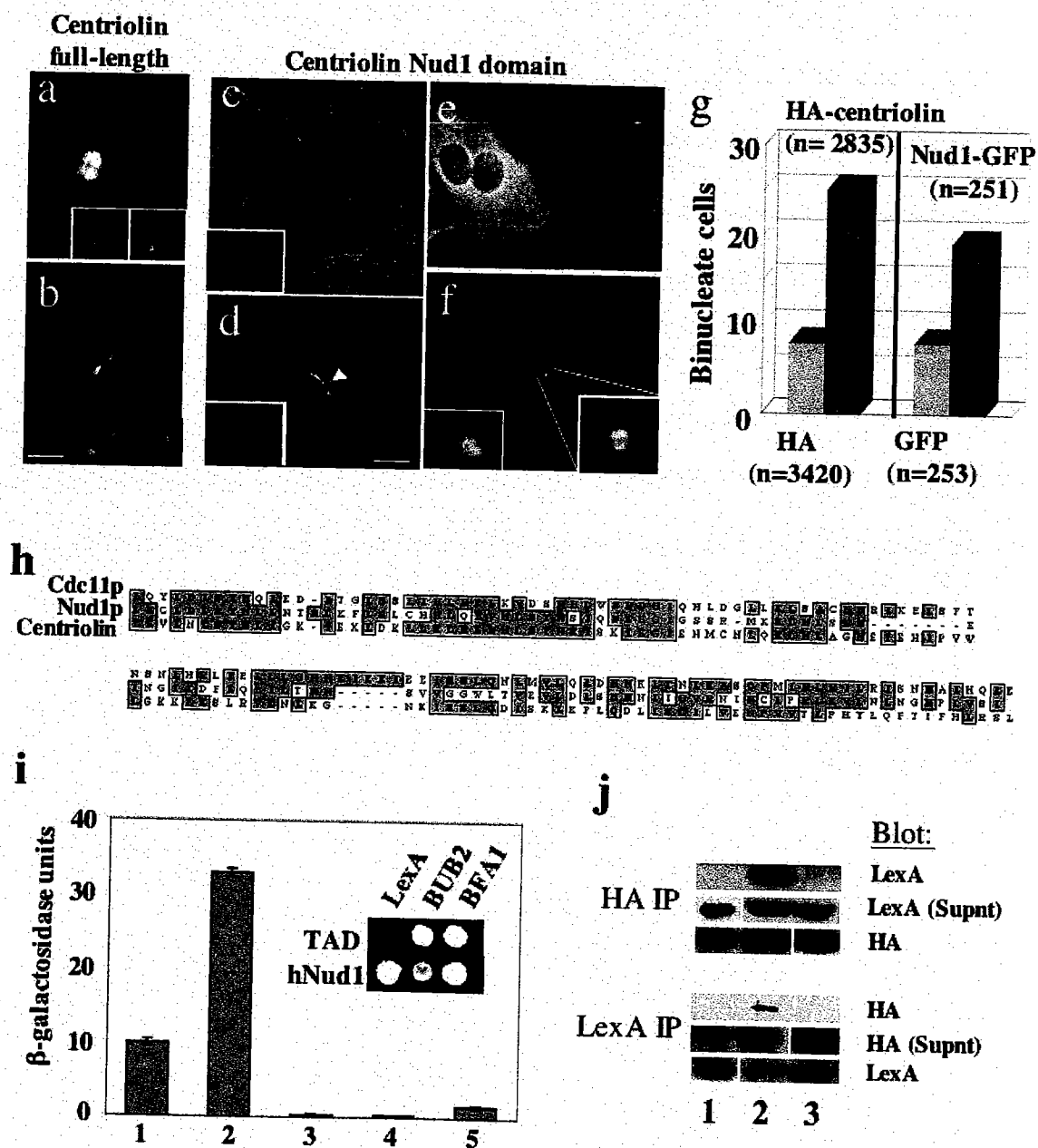


Figure 12. Cytokinesis failure in *Xenopus* embryos injected with centriolin antibodies. (a) *Xenopus* two cell embryos injected into one cell with ~50 nl anticentriolin antibodies (2 mg/ml affinity purified) fail to cleave (arrows), whereas noninjected cells (side opposite arrows) and cells injected with control rabbit IgG (2 mg/ml, top) cleave normally. (b and c) Immunofluorescence images showing two microtubule asters near a single nucleus (N) in a cell from an embryo injected with control IgG (b), and two nuclei and two asters in a cell from a centriolin antibody-injected cell (c, microtubules stained with anti- α -tubulin). Bar, 10 μ m (for b and c). (d) Quantification of results from injection experiments showing an approximately eight fold increase in cleavage failure (representative of three experiments). n, number of embryos examined. Irina Groisman contributed figure a, and Adam Gromley contributed the rest.

FIGURE 12

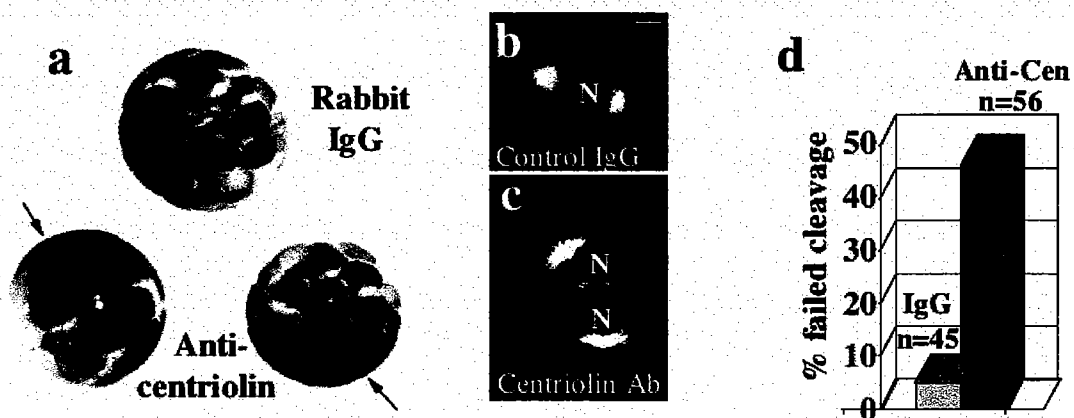
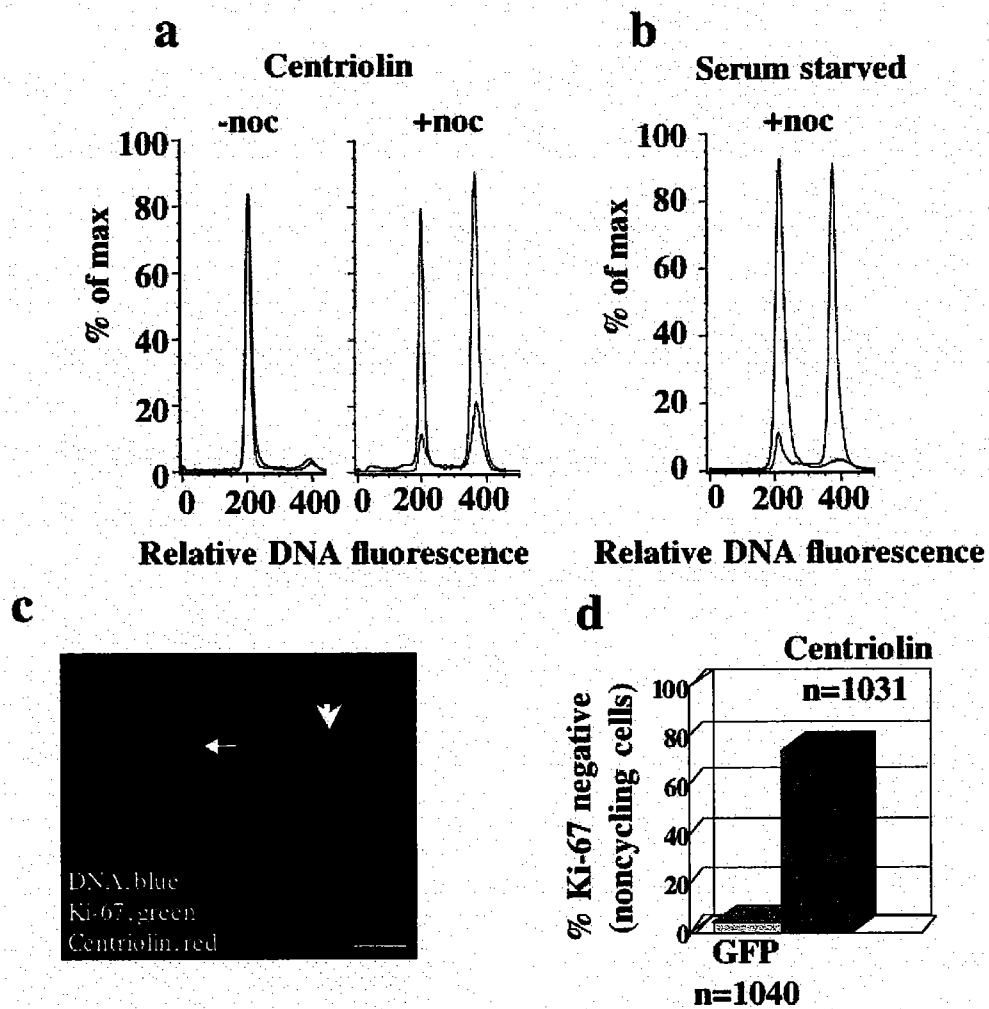


Figure 13. siRNAs targeting centriolin induces G1/G0 arrest.

(a) RPE-1 cells treated with centriolin siRNAs (blue) do not shift into the G2/M peak after nocodazole treatment as seen for control lamin siRNA-treated cells (red). (b) The inability of cells treated with centriolin siRNAs to shift into the G2/M peak is similar to that observed in serum-starved cells (blue, serum starved; red, not starved). (c) Ki-67 staining of control cells (left cell, green) occurs together with centriolin staining (left cell, red at arrow); both are gone in centriolin siRNA-treated cells (right, arrowhead). Bar, 7.5 μm . (d) Cells treated with siRNAs targeting centriolin lack Ki-67 staining (~70%), whereas most control cells stain positively (GFP siRNAs). a, b, and d are representative experiments from five experiments for a, two for b, and three for d. n, total number cell counted. Adam Gromley contributed figure d, and Agata Jurczyk contributed the rest.

FIGURE 13



Chapter III

**Pericentrin is Required for the Final Stages of
Cytokinesis and Entry into S Phase Through Its
Association with Centriolin**

Abstract

Centrosomes serve as microtubule organizing centers of animal cells and they also play a role in cytokinesis and cell cycle progression. However, the molecular pathway implicating centrosomes in cytokinesis has not been described. Previously we identified a novel centriole protein called centriolin that is required for the final stage of cytokinesis. Here we show the centrosome protein pericentrin B localizes to the region of contractile ring during early stages of cytokinesis and later to the midbody. At the midbody and at the centrosome, pericentrin B co-localizes with centriolin and both proteins show codependency for their centrosome localization. Centriolin and pericentrin interact biochemically and produce indistinguishable phenotypes upon protein depletion. Disruption of pericentrin B by RNAi results in late stage cytokinesis defects identical to the ones observed for centriolin knockdowns. In addition, in cells with an intact p53 pathway, pericentrin depletion results in G0/G1 arrest indistinguishable from centriolin silencing. Recently centriolin was shown to interact with the members of exocyst and SNARE complexes, which are required for exocytosis and completion of cytokinesis. We show that pericentrin B co-localizes with endobrevin, a member of SNARE complex, at the unique midbody ring. We conclude that pericentrin B, centriolin and the membrane secretion and fusion proteins are necessary for the final stages of cytokinesis and cell cycle progression.

Introduction

Centrosomes are responsible for organizing interphase microtubules and mitotic spindles. They have been also implicated in cytokinesis and cell cycle progression. Cells lacking centrosome exhibited defects in cytokinesis and in progression through the subsequent cell cycle (Hinchcliffe et al., 2001; Piel et al., 2001). Depletion of one of the centrosome protein, centriolin, resulted in similar phenotype as was observed in the cells that lacked centrosomes entirely. Both RPE-1 and HeLa cells treated with centriolin siRNA had difficulty completing the final steps of cytokinesis. After the contractile ring was assembled, almost 50 % of the cells remained connected by a thin intracellular bridge (Gromley et al., 2003). Subsequently, depending on their p53 status, the cells either became multinucleated and died, or if their p53 pathway was intact, they arrested in G1.

The cytokinesis defect observed in centriolin knockdowns took place in the late stages of cytokinesis, since the ingression of the contractile ring appeared to be normal (Gromley et al., 2003). Other proteins that were shown to be required during late stages of cytokinesis include members of the vesicular trafficking and membrane fusion proteins. Interestingly, centriolin has been shown to interact with the members of exocyst and SNARE complexes, which are required for exocytosis and completion of cytokinesis (Gromely, 2004). Our most recent work demonstrate the involvement of both exocyst and SNARE complexes in cytokinesis in mammalian cells, since disruption of either of their members by siRNA result in late stage cytokinesis defects (Low et al., 2003; Gromely, 2004). Moreover, this study identified a new, unique ring structure in the

midbody of animal cell composed of the centrosome protein centriolin and members of the exocyst and SNARE complexes. The cytokinesis defects seen upon depletion of any of the ring structure members resulted in indistinguishable late stage cytokinesis defects. In addition, disruption of the exocyst components resulted in accumulation of SNARE vesicles at the midbody (Gromely, 2004). This study brought together the centrosome proteins and the vesicle secretion and fusion machinery and showed their importance in cytokinesis.

The results presented in this chapter show that centriolin interacts with another centrosome protein, pericentrin B, which when depleted results in cytokinesis defect and cell cycle arrest indistinguishable from centriolin silencing. Pericentrin B also localizes during cytokinesis to the same ring structure as was shown for centriolin. Moreover, Pericentrin B additionally localizes to the membrane around the contractile ring earlier during cytokinesis. We also show that pericentrin B and centriolin interact biochemically and are co-dependant for their centrosome localization. It remains to be shown what is the relationship between pericentrin B, centriolin and the vesicular trafficking proteins during cytokinesis. Are they dependent on each other for the midbody localization, does pericentrin B interact with the members of the vesicular trafficking machinery as centriolin does?

Results and Discussion

Pericentrin B localization to the contractile ring and the midbody during cytokinesis

The localization of pericentrin A/B and B throughout the cell cycle in mammalian cells has been shown previously (Doxsey et al., 1994; Flory et al., 2000). However, in this study we discovered an additional localization for pericentrin B that has not been reported before. Here we used high resolution deconvolution microscopy to show that pericentrin B localizes to the sites of furrow constrictions, probably where the actinomyosin ring resides, during the early stages of cytokinesis (Fig. 14 A top). Later, when the furrow is much thinner, pericentrin B localizes to the midbody (Fig. 14 A bottom). This localization is specific for pericentrin B, since it was detected with an antibody specific for the C-terminus of pericentrin B which is not found in pericentrin A (Flory et al., 2000). So far, there is no antibody specific for the smaller isoform of pericentrin, pericentrin A, due to homology between pericentrin A and B throughout the entire pericentrin A sequence (Flory and Davis, 2003).

Pericentrin B exhibits co-dependency with centriolin at the centrosome and co-localizes with it at the midbody

High resolution deconvolution microscopy was used to check the centrosome localization of centriolin in RPE1 cells treated with siRNA specific for pericentrin B (Jurczyk et al., 2004). The cells with reduced levels of pericentrin B at the centrosome (77%, n=1000) also had reduced levels of centriolin (Fig. 15 A arrow). Moreover in the cells treated with centriolin siRNA both centriolin and pericentrin B were mislocalized from the

centrosome (Fig. 15 B arrow). The cells with normal levels of pericentrin B and centriolin served as controls (Fig. 15 A, bottom and 15 B arrowheads). This data indicates that pericentrin B and centriolin show co-dependency in their centrosome localization.

We also looked to see if pericentrin B and centriolin are co-localized during cytokinesis. In the early stages of cytokinesis, when pericentrin B seemed to mark the membrane around contractile ring, centriolin did not localize to any of the pericentrin B containing spots. However, later, when the midbody was thinner, both centriolin and pericentrin B partially co-localized to the midbody (Fig. 15 C). These results show that pericentrin B and centriolin co-localize to the midbody ring structure in the late stages of cytokinesis.

Pericentrin and centriolin interact biochemically

To test if pericentrin and centriolin interact biochemically, we co-precipitated endogenous centriolin using pericentrin A/B antibody and in a reciprocal experiment, we co-precipitated pericentrin using centriolin antibody (Fig. 16 A). We observed no co-immunoprecipitation of any of the proteins when the antibody was omitted (Fig. 16 A, Beads (Bd)). Lysates (Lys) from the immunoprecipitations experiments are indicated. These data show that pericentrin B interacts with centriolin. It remains to be shown if these interactions are direct.

Pericentrin B co-localizes with endobrevin at the midbody ring during cytokinesis

In the light of recent data showing the involvement of SNARE components and the exocyst complex in the final stage of cytokinesis and their co-localization to the centriolin ring (Gromely, 2004; Low et al., 2003), we tested to see if pericentrin B can co-localize with endobrevin, the member of SNARE complex. We showed that in the earlier stages of cytokinesis pericentrin B was localized to the ring and partially co-localized with endobrevin to both sides of the midbody (Fig. 17 A, enlargement below as indicated by square in the images above). Therefore, pericentrin B localizes to the midbody ring before endobrevin does, just as was shown for centriolin (Gromely, 2004). During later stages of cytokinesis, when the intercellular bridge was much thinner, pericentrin B partially co-localized with endobrevin to the ring and very weakly along both sides of the midbody (Fig. 17 B).

Pericentrin B RNAi induces a late stage cytokinesis defects

When pericentrin B was depleted using a specific siRNA (Jurczyk et al., 2004) it resulted in cells that remained connected by thin intercellular bridges and a very small increase in binucleate cells (Fig. 18 A right-binucleate cell, left-thin bridge connection). Forty two percent of RPE1 cells treated with pericentrin B siRNA for 14 h showed this phenotype as compared with 5% of the control, GFP siRNA treated cells (Fig. 18 B). Moreover, in HeLa cells we observed an increased number of telophase cells (3.9% for GFP control and 10% for pericentrin B knockdowns) in addition to cells connected by thin intercellular bridges. These data show that disruption of pericentrin B produces a

phenotype indistinguishable from centriolin (Gromley et al., 2003) and implicates the involvement of pericentrin B in the final stages of cytokinesis.

Pericentrin B disruption causes G0/G1 arrest

The cytokinesis defects observed in pericentrin B knockdowns were observed at early times after siRNA treatment (14-17 h). At later times (48-72 h) a reduction in the mitotic index was observed in RPE1 cells, suggesting that the cells were arrested at some other stage of the cell cycle. To determine at which cell cycle stage the cells were arrested, we treated pericentrin B knockdowns with nocodazole to induce mitotic arrest. In the presence of nocodazole, control cells showed a significant shift from the G1 peak to the G2/M peak (Fig. 19 A, red). In contrast cell treated with siRNAs targeting pericentrin B did not significantly shift into the G2/M peak in the presence of nocodazole but remained largely in G1 (Fig. 19 A, blue). The proportion of cells in S phase was unaltered in cells silenced for pericentrin B both in the presence of nocodazole (pericentrin B, 14%; lamin, 19 %) or in the absence (pericentrin B, 13%; lamin 23%). Cells treated with pericentrin B siRNA showed a similar pattern of cell cycle distribution as serum starved, G0 cells (Fig. 19 B, serum starved, blue; GFP control, red). These results demonstrate that cells with reduced pericentrin arrest before S phase. To further determine the time of arrest we used Ki-67 antibody staining. Ki-67 is an antibody directed against a nuclear protein that stains cycling cells or cells arrested in G1/S and S, but not cells that are quiescent (G0) or differentiated (Gerdes et al., 1984). As expected, nearly all untreated RPE1 cells or control cells treated with siRNAs targeting GFP or lamin A/C were positive for Ki-67

(Fig. 19 C). However, most cells with reduced pericentrin B had undetectable levels of Ki-67 staining (Fig. 5 C). This arrest was previously shown for centriolin (Gromley et al., 2003) and it does not occur in cells with an abrogated p53 pathway, such as HeLa, or Saos-2 (Fig. 19 D). G1 arrest was also observed in cells whose centrosome was removed by either laser ablation or microsurgery (Hinchcliffe et al., 2001; Khodjakov and Rieder, 2001). Therefore, either centrosome damage by depletion of its core components or cytokinesis failure could result in cell cycle arrest.

Figure 14. Pericentrin B localization to the contractile ring and the midbody during cytokinesis.

(A, top) High resolution deconvolution images showing pericentrin B localization to the area of contractile ring formation during early cytokinesis and to the midbody during late stages of cytokinesis (bottom). Overlay with pericentrin B (PcntB, red) α -tubulin (green) and DNA (blue).

FIGURE 14

A

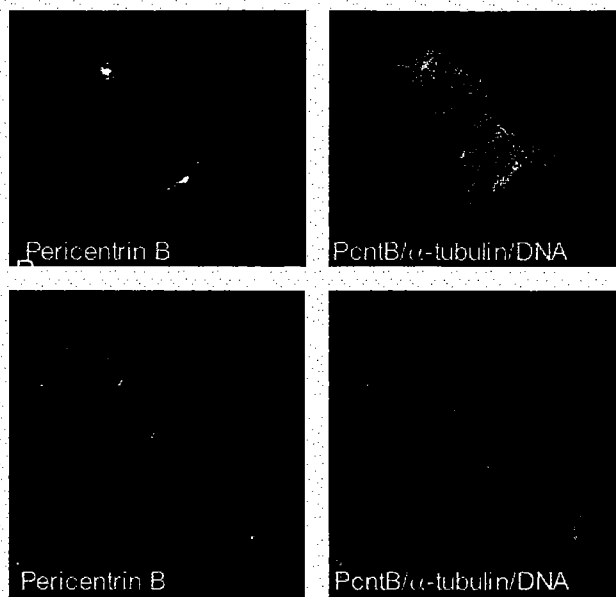


Figure 15. Pericentrin B exhibits co-dependency with centriolin at the centrosome and co-localizes with it at the midbody.

(A) High resolution deconvolution images of RPE1 cells treated with pericentrin A siRNA. The cell with reduced levels of pericentrin B at the centrosome (arrow) also had reduced levels of centriolin. (B) High resolution deconvolution images of RPE1 cells treated with centriolin siRNA. The cells with reduced levels of centriolin at the centrosome (arrow) also had reduced levels of pericentrin B. The cells with normal levels of both proteins (arrowhead) served as controls. Merge showing pericentrin B (red), centriolin (green), DNA (blue). (C) High resolution deconvolution images of HeLa cells showing that pericentrin B and centriolin co-localize at the midbody ring during cytokinesis. Enlargement of the midbody ring (arrow) in the right corner of each picture. Pericentrin B (red), centriolin (green).

FIGURE 15

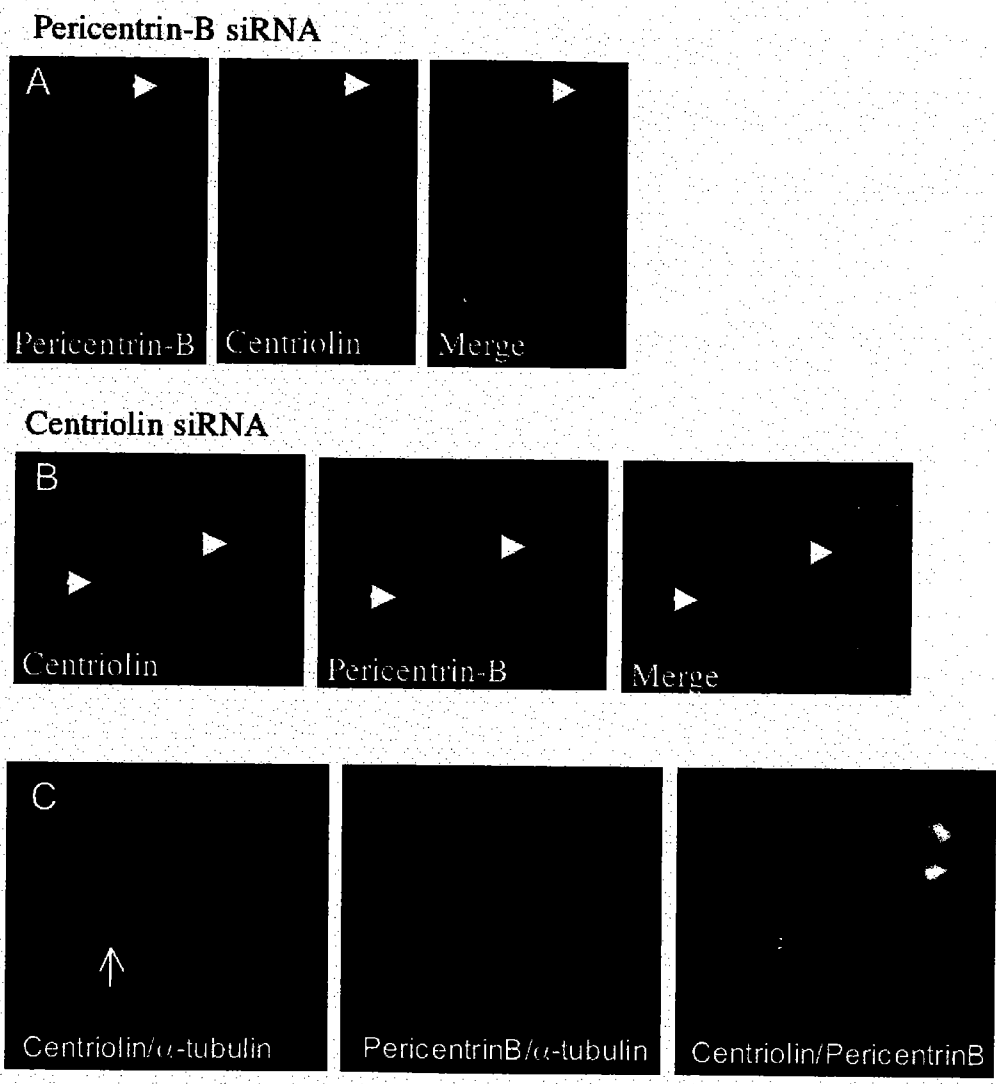


Figure 16. Pericentrin and centriolin interact biochemically.

(A) Endogenous centriolin and pericentrin interact with each other when immunoprecipitated from mitotic RPE1 cells. The pericentrin antibody used in this experiment recognizes pericentrin A and B and is raised to the amino-terminal region of pericentrin (PcN). No co-immunoprecipitation was observed when the antibodies were omitted in beads control (Bd). Lysates (Lys) are indicated. All of the immunoprecipitations were loaded and 7% of the immunoprecipitations were loaded for the lysates.

FIGURE 16

A

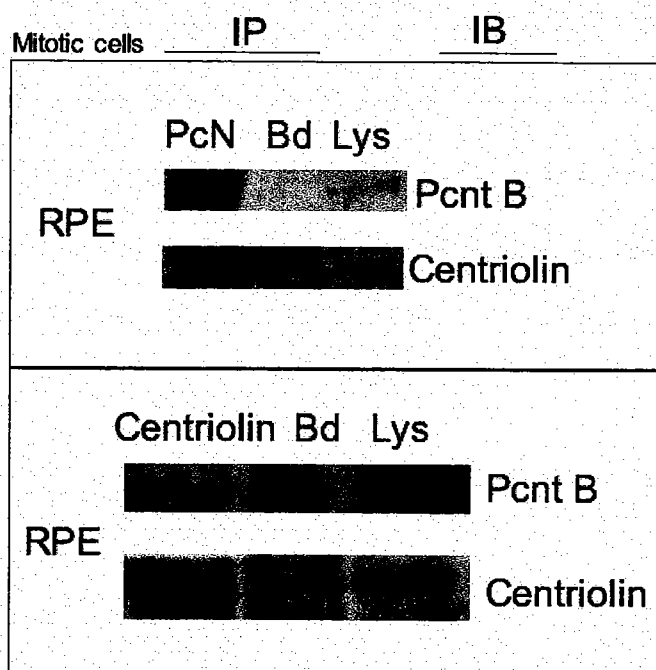


Figure 17. Pericentrin B co-localizes with endobrevin at the midbody ring during cytokinesis.

(A) High resolution deconvolution images showing pericentrin B and endobrevin localization during early stages of cytokinesis. Pericentrin B localizes to the midbody ring and partially co-localized with endobrevin to both sides of the midbody. (below) overlay showing enlargement of the midbody with pericentrin B (green) and endobrevin (red). (B) High resolution deconvolution images showing pericentrin B and endobrevin localization during late stages of cytokinesis. Pericentrin B co-localized with endobrevin to the midbody ring and very weakly along both sides of the midbody. (below) overlay of endobrevin and pericentrin B. Enlargement of the midbody ring in the right corner of each picture. Endobrevin (green), pericentrin B (red).

FIGURE 17

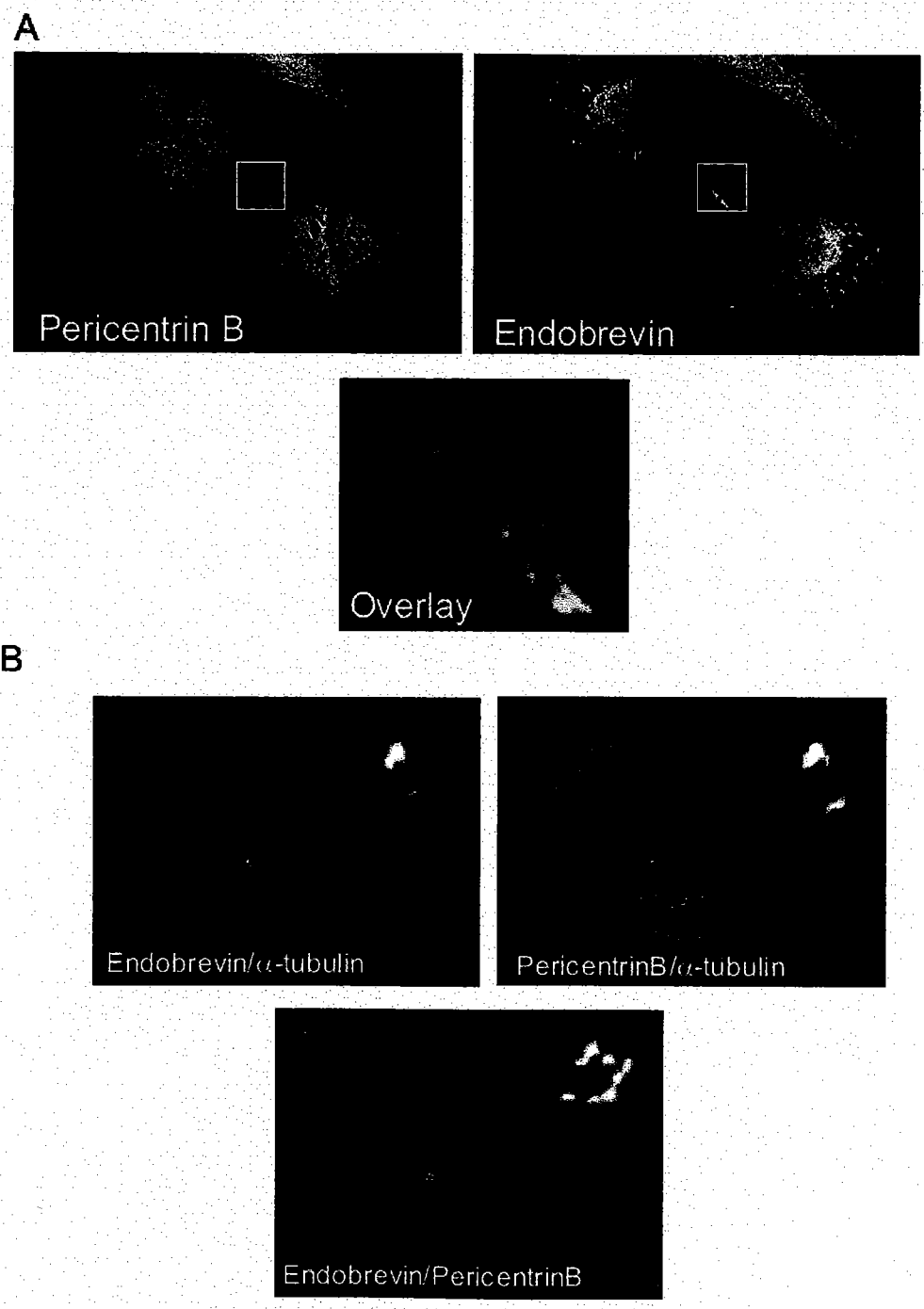
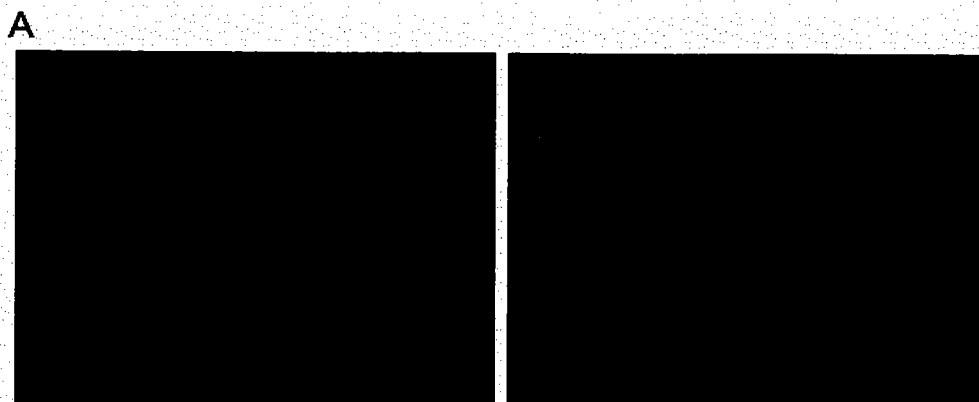


Figure 18. Pericentrin B RNAi induces a late stage cytokinesis defects.

(A) High resolution deconvolution images from RPE1 cells after 14 h of pericentrin B siRNA treatment showing cytokinesis defects, (left) shows an example of binucleate cell undergoing cytokinesis, the midbody is still visible, (right) thin intercellular bridge connections that represent most of the counted defects. (B) Quantatization of the images shown in (A), Abnormal/telophase/multinucleated cells are percent of total cells counted (n=1000).

FIGURE 18



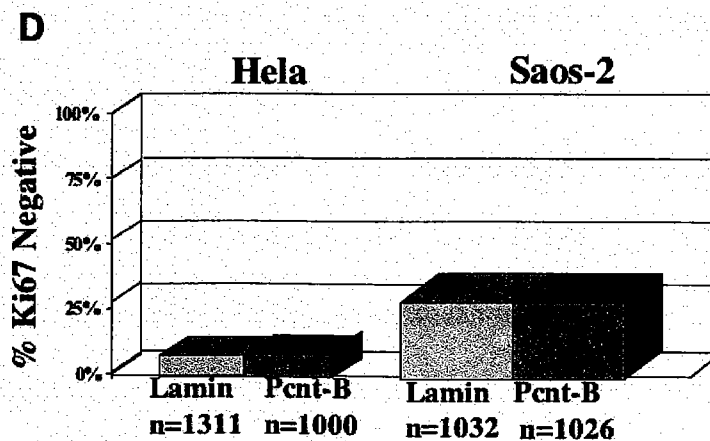
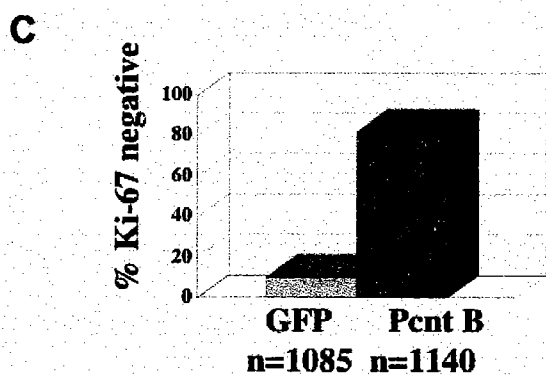
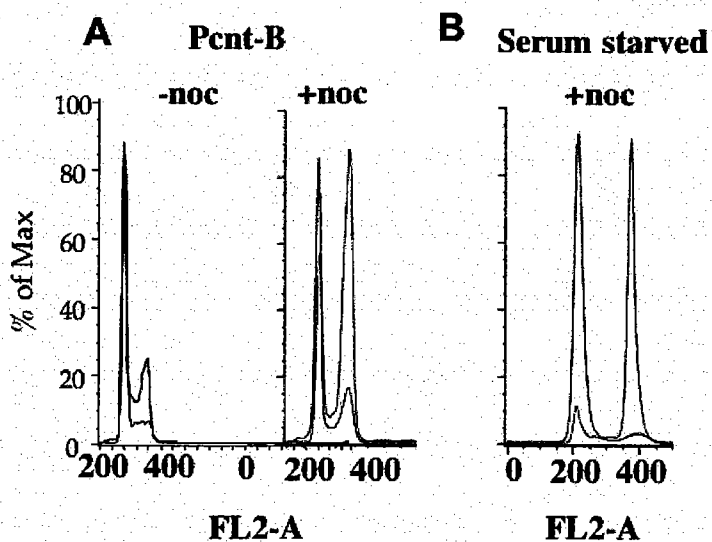
B

<u>siRNA</u>	<u>Abn. Telophase/multinucleated</u>
Pericentrin B	42%
GFP	5%

Figure 19. Pericentrin B disruption causes G0/G1 arrest.

(A) RPE1 cells treated with centriolin pericentrin B siRNAs (blue) do not shift into the G2/M peak after nocodazole treatment as seen for control lamin siRNA-treated cells (red). (B) The inability of cells treated with pericentrin B siRNAs to shift into the G2/M peak is similar to that observed in serum-starved cells (blue, serum starved; red, not starved). (C) Cells treated with siRNA targeting pericentrin B lack Ki-67 staining (~80%), whereas most control cells stain positively (GFP siRNA). (D) HeLa and Saos-2 cells defective in the p53 pathway treated with siRNA targeting pericentrin B stained positively for Ki-67 just as controls (lamin A/C).

FIGURE 19



DISCUSSION

In this dissertation, I present the requirement of two centrosome proteins: pericentrin and centriolin for cytokinesis and cell cycle progression. Moreover I show that pericentrin is also involved in ciliogenesis. Centriolin is a novel centriolar protein which localizes to the subdistal appendages of mother centriole. Both pericentrin and centriolin interact biochemically and show identical phenotypes upon siRNA treatment. It remains to be shown how these two proteins can function in so many different cellular processes at multiple sites in the cell, especially knowing that they are so rare (Doxsey et al., 1994; Flory and Davis, 2003; Gromley et al., 2003).

One common denominator to both cilia formation and cytokinesis is the requirement of new membrane generation and involvement of vesicle targeting and fusion machinery. As a matter of fact, the exocyst complex, which is necessary for vesicle targeting, has been localized to both primary cilia and midbody ring structure during cytokinesis (Gromely, 2004; Rogers et al., 2004). Members of the *S. cerevisiae* exocyst complex have been shown to localize to the mother-bud neck during cytokinesis (Finger et al., 1998) and to the actomyosin contractile ring in *S. pombe* (Wang et al., 2002b). So far only one study showed the exocyst complex localization to the cilia (Rogers et al., 2004), therefore, it would be of interest to determine its localization in pericentrin B knockdowns that do not form primary cilia. During ciliogenesis vesicles were shown to

appear at the distal end of the basal body. Later, the vesicle enclosing the ciliary bud fuses with the plasma membrane and the cilium is seen at the plasma membrane (Sorokin, 1968). If exocystic vesicles are involved in ciliogenesis, one could predict they should accumulate near the basal body, just as they accumulated around the midbody during cytokinesis in cells with reduced centriolin levels (Gromely, 2004). In addition, centriolin which already was shown to interact with both SNARE and exocyst complexes (Gromely, 2004) also inhibits primary cilia formation upon protein depletion (Jurczyk and Doxsey, unpublished observation). Additional work needs to be performed in order to define the relationship between cytokinesis and ciliogenesis, however these processes may have more in common than we originally thought.

Primary cilia are formed from the maternal centriole of the centrosome in cycling and non-cycling cells (Rieder et al., 2001; Rieder et al., 1979). This suggests that these two structures may have shared components and functions. In fact, our data show that the centrosome protein pericentrin also localizes to the centrioles/basal bodies of primary cilia and affects primary cilia function. Moreover, IFT proteins (Iomini et al., 2004) are found at centrosomes in interphase cells and spindle poles and microtubules during mitosis. In addition IFTs are found in isolated centrosome preparations from cycling cells (Jurczyk et al., 2004). Thus, it is possible that pericentrin, IFT proteins and PC2 cooperate in functions at the centrosome. For example, IFT proteins may be involved in the microtubule-based or mitotic functions of pericentrin. Alternatively, IFTs and pericentrin could utilize the same molecular motor-driven pathway to assemble onto

centrosomes, rather than independent pathways as we suggested (Zimmerman and Doxsey, 2000). It is also possible that the centrosome localization of IFT proteins simply ensures that they will ultimately be localized to the base of primary cilia. Centrosomal PC2 may play a role in calcium signaling at the centrosome in much the way that it does in primary cilia. Additional studies will be required to elucidate the role of IFT proteins and PC2 at centrosomes and spindle poles and to determine the significance of a potential interaction between pericentrin, IFT proteins and PC2 at these sites.

The interactions of pericentrin with PC2 and IFT proteins in ciliated cells suggest a role for pericentrin in anchoring multiple proteins involved in calcium signaling. Consistent with this idea is the observation that pericentrin binds the cyclic AMP-activated protein kinase A (PKA) (Diviani et al., 2000), and that cAMP regulates cyst formation in polycystic kidney disease (Hanaoka and Guggino, 2000). Pericentrin B also has a calmodulin domain (Flory et al., 2000) that could modulate protein function through calcium at centrioles. Additional studies will be required to elucidate the precise role of pericentrin in anchoring calcium-signaling molecules at primary cilia.

An important issue that needs to be clarified in the pericentrin field is the relationship between the different isoforms of pericentrin. Currently, we have antibodies specific for only one isoform, pericentrin B, and this antibody is useful only for immunofluorescence analysis (Flory et al., 2000). There is no antibody specific for pericentrin A due to homology with pericentrin B throughout the whole pericentrin A sequence (Flory and

Davis, 2003; Zimmerman, 2004). RNAi technology already gave us some idea that there are differences between pericentrin A and B in both their localizations and functions. Targeting the originally identified form of pericentrin (pericentrin A) by RNAi reduction, overexpression and antibody inhibition affects microtubule organization and mitosis in vertebrates (Doxsey et al., 1994; Pihan et al., 2001; Purohit et al., 1999; Zimmerman et al., 2004). On the other hand, targeting pericentrin B or its orthologues by RNAi depletion does not seem to affect microtubule organization or mitosis (Dammerrmann and Merdes, 2002; Martinez-Compos et al., 2004; Zimmerman et al., 2004), but it does affect *Xenopus* aster formation and ciliogenesis (Jurczyk et al., 2004; Kawaguchi and Zheng, 2003; Takahashi et al., 2002). Thus, it is likely that pericentrin and other pericentrin/AKAP450-related proteins represent a family of multifunctional scaffold proteins that bind many protein and activities, and perform multiple independent and overlapping functions

The cell cycle arrest observed when pericentrin, centriolin and other centrosome proteins were depleted needs to be further characterized. Our data so far indicates that this arrest could be a novel checkpoint that monitors “centrosome integrity”, however, what the checkpoint monitors remains an open question. The arrest seems to depend on an intact p53 pathway, since HeLa or SaOS cells that are defective in this pathway do not arrest upon centrosome protein depletion (Gromley et al., 2003; Chapter III). It is possible that the “centrosome integrity” checkpoint senses a change in phosphorylation status of one of the core centrosome proteins. γ -Tubulin would be a good candidate to study, since most

of the centrosome protein knockdowns did not have any effect on γ -tubulin localization (Gromley et al., 2003; Dammermann and Merdes, 2002).

References

- Abaza, A., J.M. Soleilhac, J. Westendorf, M. Piel, I. Crevel, A. Roux, and F. Pirollet. 2003. M phase phosphoprotein 1 is a human plus-end-directed kinesin-related protein required for cytokinesis. *J Biol Chem.* 278:27844-52.
- Adams, R.R., M. Carmena, and W.C. Earnshaw. 2001. Chromosomal passengers and the (aurora) ABCs of mitosis. *Trends Cell Biol.* 11:49-54.
- Andersen, S.S. 2000. Spindle assembly and the art of regulating microtubule dynamics by MAPs and Stathmin/Op18. *Trends Cell Biol.* 10:261-7.
- Andreassen, P.R., O.D. Lohez, F.B. Lacroix, and R.L. Margolis. 2001. Tetraploid State Induces p53-dependent Arrest of Nontransformed Mammalian Cells in G1. *Mol Biol Cell.* 12:1315-28.
- Balczon, R., L. Bao, and W.E. Zimmer. 1994. PCM-1, A 228-kD centrosome autoantigen with a distinct cell cycle distribution. *J Cell Biol.* 124:783-93.
- Bardin, A.J., and A. Amon. 2001. Men and sin: what's the difference? *Nat Rev Mol Cell Biol.* 2:815-26.
- Bardin, A.J., R. Visintin, and A. Amon. 2000. A mechanism for coupling exit from mitosis to partitioning of the nucleus. *Cell.* 102:21-31.
- Beites, C.L., H. Xie, R. Bowser, and W.S. Trimble. 1999. The septin CDCrel-1 binds syntaxin and inhibits exocytosis. *Nat Neurosci.* 2:434-9.
- Bischoff, J.R., and G.D. Plowman. 1999. The Aurora/Ipl1p kinase family: regulators of chromosome segregation and cytokinesis. *Trends Cell Biol.* 9:454-9.
- Blomberg, M., and S.J. Doxsey. 1998. Rapid isolation of centrosomes. *Meth. Enzymol.* 298:228-238.
- Bobinnec, Y., A. Khodjakov, L.M. Mir, C.L. Rieder, C.L. Edde, and M. Bornens. 1998. Centriole disassembly in vivo and its effect on centrosome structure and function in vertebrate cells. *J. Cell Biol.* 143:1575-1589.
- Boman, A.L., J. Kuai, X. Zhu, J. Chen, R. Kuriyama, and R.A. Kahn. 1999. Arf proteins bind to mitotic kinesin-like protein 1 (MKLP1) in a GTP-dependent fashion. *Cell Motil Cytoskeleton.* 44:119-32.

- Bornens, M. 2002. Centrosome composition and microtubule anchoring mechanisms. *Curr Opin Cell Biol.* 14:25-34.
- Boveri, T. 1914. Williams and Wilkins, Baltimore.
- Brazelton, W.J., C.D. Amundsen, C.D. Silflow, and P.A. Lefebvre. 2001. The bld1 mutation identifies the *Chlamydomonas osm-6* homolog as a gene required for flagellar assembly. *Curr Biol.* 11:1591-4.
- Burton, K., and D.L. Taylor. 1997. Traction forces of cytokinesis measured with optically modified elastic substrata. *Nature.* 385:450-4.
- Carter, S.B. 1967. Effects of cytochalasins on mammalian cells. *Nature.* 213:261-4.
- Carvalho, A., M. Carmena, C. Sambade, W.C. Earnshaw, and S.P. Wheatley. 2003. Survivin is required for stable checkpoint activation in taxol-treated HeLa cells. *J Cell Sci.* 116:2987-98.
- Cole, D.G., D.R. Diener, A.L. Himelblau, P.L. Beech, J.C. Fuster, and J.L. Rosenbaum. 1998. *Chlamydomonas* kinesin-II-dependent intraflagellar transport (IFT): IFT particles contain proteins required for ciliary assembly in *Caenorhabditis elegans* sensory neurons. *J Cell Biol.* 141:993-1008.
- Compton, D.A. 1998. Focusing on spindle poles. *J. Cell Sci.* 111:1377-1481.
- Cuif, M.H., F. Possmayer, H. Zander, N. Bordes, F. Jollivet, A. Couedel-Courteille, I. Janoueix-Lerosey, G. Langsley, M. Bornens, and B. Goud. 1999. Characterization of GAPCenA, a GTPase activating protein for Rab6, part of which associates with the centrosome. *Embo J.* 18:1772-82.
- Dammermann, A., and A. Merdes. 2002. Assembly of centrosomal proteins and microtubule organization depends on PCM-1. *J Cell Biol.* 159:255-66.
- Deane, J.A., D.G. Cole, E.S. Seeley, D.R. Diener, and J.L. Rosenbaum. 2001. Localization of intraflagellar transport protein IFT52 identifies basal body transitional fibers as the docking site for IFT particles. *Curr Biol.* 11:1586-90.
- Dicthenberg, J., W. Zimmerman, C. Sparks, A. Young, C. Vidair, Y. Zheng, W. Carrington, F. Fay, and S.J. Doxsey. 1998. Pericentrin and gamma tubulin form a protein complex and are organized into a novel lattice at the centrosome. *J. Cell Biol.* 141:163-174.

- Diviani, D., L.K. Langeberg, S.J. Doxsey, and J.D. Scott. 2000. Pericentrin anchors protein kinase A at the centrosome through a newly identified RII-binding domain. *Curr Biol.* 10:417-20.
- Doxsey, S. 2002. Duplicating dangerously: linking centrosome duplication and aneuploidy. *Mol Cell.* 10:439-40.
- Doxsey, S.J. 2001. Centrosomes as command centres for cellular control. *Nat Cell Biol.* 3:E105-8.
- Doxsey, S.J., P. Stein, L. Evans, P. Calarco, and M. Kirschner. 1994. Pericentrin, a highly conserved protein of centrosomes involved in microtubule organization. *Cell.* 76: 639-650.
- Elbashir, S.M., J. Harborth, W. Lendeckel, A. Yalcin, K. Weber, and T. Tuschl. 2001. Duplexes of 21-nucleotide RNAs mediate RNA interference in cultured mammalian cells. *Nature.* 411:494-8.
- Field, C.M., and D. Kellogg. 1999. Septins: cytoskeletal polymers or signalling GTPases? *Trends Cell Biol.* 9:387-94.
- Finger, F.P., T.E. Hughes, and P. Novick. 1998. Sec3p is a spatial landmark for polarized secretion in budding yeast. *Cell.* 92:559-71.
- Finger, F.P., and J.G. White. 2002. Fusion and fission: membrane trafficking in animal cytokinesis. *Cell.* 108:727-30.
- Fire, A., S. Xu, M.K. Montgomery, S.A. Kostas, S.E. Driver, and C.C. Mello. 1998. Potent and specific genetic interference by double-stranded RNA in *Caenorhabditis elegans*. *Nature.* 391:806-11.
- Flory, M.R., and T.N. Davis. 2003. The centrosomal proteins pericentrin and kendrin are encoded by alternatively spliced products of one gene. *Genomics.* 82:401-5.
- Flory, M.R., M. Morpew, J.D. Joseph, A.R. Means, and T.N. Davis. 2002. Pcp1p, an Spc110p-related calmodulin target at the centrosome of the fission yeast *Schizosaccharomyces pombe*. *Cell Growth Differ.* 13:47-58.
- Flory, M.R., M.J. Moser, R.J. Monnat, Jr., and T.N. Davis. 2000. Identification of a human centrosomal calmodulin-binding protein that shares homology with pericentrin. *Proc Natl Acad Sci U S A.* 97:5919-23.

- Fontijn, R.D., B. Goud, A. Echard, F. Jollivet, J. van Marle, H. Pannekoek, and A.J. Horrevoets. 2001. The human kinesin-like protein RB6K is under tight cell cycle control and is essential for cytokinesis. *Mol Cell Biol.* 21:2944-55.
- Fry, A.M., T. Mayor, P. Meraldi, Y.D. Stierhof, K. Tanaka, and E.A. Nigg. 1998. C-Nap1, a novel centrosomal coiled-coil protein and candidate substrate of the cell cycle-regulated protein kinase Nek2. *J Cell Biol.* 141:1563-74.
- Fujiwara, K., M.E. Porter, and T.D. Pollard. 1978. Alpha-actinin localization in the cleavage furrow during cytokinesis. *J Cell Biol.* 79:268-75.
- Fujiwara, M., T. Ishihara, and I. Katsura. 1999. A novel WD40 protein, CHE-2, acts cell-autonomously in the formation of *C. elegans* sensory cilia. *Development.* 126:4839-48.
- Gassmann, R., A. Carvalho, A.J. Henzing, S. Ruchaud, D.F. Hudson, R. Honda, E.A. Nigg, D.L. Gerloff, and W.C. Earnshaw. 2004. Borealin: a novel chromosomal passenger required for stability of the bipolar mitotic spindle. *J Cell Biol.* 166:179-91.
- Gavet, O., C. Alvarez, P. Gaspar, and M. Bornens. 2003. Centrin4p, a novel mammalian centrin specifically expressed in ciliated cells. *Mol Biol Cell.* 14:1818-34.
- Gerdes, J., H. Lemke, H. Baisch, H.H. Wacker, U. Schwab, and H. Stein. 1984. Cell cycle analysis of a cell proliferation-associated human nuclear antigen defined by the monoclonal antibody Ki-67. *J Immunol.* 133:1710-5.
- Gromely, A., Yeaman, C., Redick, S., and Doxsey, S. 2004. Centriolin-anchoring of exocyst and SNARE complexes at the midbody is required for localized secretion and abscission during cytokinesis. *Submitted to Cell.*
- Gromley, A., A. Jurczyk, J. Sillibourne, E. Halilovic, M. Mogensen, I. Groisman, M. Blomberg, and S. Doxsey. 2003. A novel human protein of the maternal centriole is required for the final stages of cytokinesis and entry into S phase. *J Cell Biol.* 161:535-45.
- Gruneberg, U., K. Campbell, C. Simpson, J. Grindlay, and E. Schiebel. 2000. Nud1p links astral microtubule organization and the control of exit from mitosis. *Embo J.* 19:6475-88.
- Guasch, G., G.J. Mack, C. Popovici, N. Dastugue, D. Birnbaum, J.B. Rattner, and M.J. Pebusque. 2000. FGFR1 is fused to the centrosome-associated protein CEP110 in the 8p12 stem cell myeloproliferative disorder with t(8;9)(p12;q33). *Blood.* 95:1788-96.

- Guertin, D.A., S. Trautmann, and D. McCollum. 2002. Cytokinesis in eukaryotes. *Microbiol Mol Biol Rev.* 66:155-78.
- Gunawardane, R.N., S.B. Lizarraga, C. Wiese, A. Wilde, and Y. Zheng. 2000. gamma-Tubulin complexes and their role in microtubule nucleation. *Curr Top Dev Biol.* 49:55-73.
- Han, Y.G., B.H. Kwok, and M.J. Kernan. 2003. Intraflagellar transport is required in *Drosophila* to differentiate sensory cilia but not sperm. *Curr Biol.* 13:1679-86.
- Hanaoka, K., and W.B. Guggino. 2000. cAMP regulates cell proliferation and cyst formation in autosomal polycystic kidney disease cells. *J Am Soc Nephrol.* 11:1179-87.
- Hanaoka, K., F. Qian, A. Boletta, A.K. Bhunia, K. Piontek, L. Tsiokas, V.P. Sukhatme, W.B. Guggino, and G.G. Germino. 2000. Co-assembly of polycystin-1 and -2 produces unique cation-permeable currents. *Nature.* 408:990-4.
- Hill, E., M. Clarke, and F.A. Barr. 2000. The Rab6-binding kinesin, Rab6-KIFL, is required for cytokinesis. *Embo J.* 19:5711-9.
- Hinchcliffe, E.H. 2003. Cell cycle: seeking permission from the mother centriole. *Curr Biol.* 13:R646-8.
- Hinchcliffe, E.H., F.J. Miller, M. Cham, A. Khodjakov, and G. Sluder. 2001. Requirement of a centrosomal activity for cell cycle progression through G1 into S phase. *Science.* 291:1547-50.
- Hsu, S.C., D. TerBush, M. Abraham, and W. Guo. 2004. The exocyst complex in polarized exocytosis. *Int Rev Cytol.* 233:243-65.
- Iomini, C., K. Tejada, W. Mo, H. Vaananen, and G. Piperno. 2004. Primary cilia of human endothelial cells disassemble under laminar shear stress. *J Cell Biol.* 164:811-7.
- Ito, H., Y. Fukuda, K. Murata, and A. Kimura. 1983. Transformation of intact yeast cells treated with alkali cations. *J Bacteriol.* 153:163-8.
- Jahn, R., and T.C. Sudhof. 1999. Membrane fusion and exocytosis. *Annu Rev Biochem.* 68:863-911.
- Jurczyk, A., A. Gromely, S. Redick, J. San Augustin, G.B. Witman, G.J. Pazour, and S. Doxsey. 2004. Pericentrin is required for primary cilia assembly and anchoring of intraflagellar transport proteins at basal bodies. *J. Cell Biol.* in press.

- Kaiser, B.K., Z.A. Zimmerman, H. Charbonneau, and P.K. Jackson. 2002. Disruption of Centrosome Structure, Chromosome Segregation, and Cytokinesis by Misexpression of Human Cdc14A Phosphatase. *Mol Biol Cell*. 13:2289-300.
- Kawaguchi, S.I., and Y. Zheng. 2003. Characterization of a Drosophila centrosome protein CP309 that shares homology with Kendrin and CG-NAP. *Mol Biol Cell*.
- Keryer, G., B. Di Fiore, C. Celati, K.F. Lehtreck, M. Mogensen, A. Delouee, P. Lavia, M. Bornens, and A.M. Tassin. 2003a. Part of Ran Is Associated with AKAP450 at the Centrosome: Involvement in Microtubule-organizing Activity. *Mol Biol Cell*. 14:4260-71.
- Keryer, G., O. Witczak, A. Delouee, W.A. Kemmner, D. Rouillard, K. Tasken, and M. Bornens. 2003b. Dissociating the centrosomal matrix protein AKAP450 from centrioles impairs centriole duplication and cell cycle progression. *Mol Biol Cell*. 14:2436-46.
- Khodjakov, A., and C.L. Rieder. 2001. Centrosomes enhance the fidelity of cytokinesis in vertebrates and are required for cell cycle progression. *J Cell Biol*. 153:237-42.
- Knop, M., G. Pereira, S. Geissler, K. Grein, and E. Schiebel. 1997. The spindle pole body component Spc97p interacts with the gamma-tubulin of *Saccharomyces cerevisiae* and functions in microtubule organization and spindle pole body duplication. *Embo J*. 16:1550-64.
- Knop, M., and E. Schiebel. 1997. Spc98p and Spc97p of the yeast gamma-tubulin complex mediate binding to the spindle pole body via their interaction with Spc110p. *Embo J*. 16:6985-95.
- Kochanski, R.S., and G.G. Borisy. 1990. Mode of centriole duplication and distribution. *J Cell Biol*. 110:1599-605.
- Kohl, L., D. Robinson, and P. Bastin. 2003. Novel roles for the flagellum in cell morphogenesis and cytokinesis of trypanosomes. *Embo J*. 22:5336-5346.
- Kozminski, K.G., P.L. Beech, and J.L. Rosenbaum. 1995. The *Chlamydomonas* kinesin-like protein FLA10 is involved in motility associated with the flagellar membrane. *J Cell Biol*. 131:1517-27.
- Kozminski, K.G., K.A. Johnson, P. Forscher, and J.L. Rosenbaum. 1993. A motility in the eukaryotic flagellum unrelated to flagellar beating. *Proc Natl Acad Sci U S A*. 90:5519-23.

- Kubo, A., H. Sasaki, A. Yuba-Kubo, S. Tsukita, and N. Shiina. 1999. Centriolar satellites: molecular characterization, ATP-dependent movement toward centrioles and possible involvement in ciliogenesis. *J Cell Biol.* 147:969-80.
- Lange, B.M., and K. Gull. 1995. A molecular marker for centriole maturation in the mammalian cell cycle. *J. Cell Biol.* 130:919-927.
- Lee, M.J., F. Gergely, K. Jeffers, S.Y. Peak-Chew, and J.W. Raff. 2001. Msp/XMAP215 interacts with the centrosomal protein D-TACC to regulate microtubule behaviour. *Nat Cell Biol.* 3:643-9.
- Lens, S.M., R.M. Wolthuis, R. Klompmaker, J. Kauw, R. Agami, T. Brummelkamp, G. Kops, and R.H. Medema. 2003. Survivin is required for a sustained spindle checkpoint arrest in response to lack of tension. *Embo J.* 22:2934-47.
- Li, F., E.J. Ackermann, C.F. Bennett, A.L. Rothermel, J. Plescia, S. Tognin, A. Villa, P.C. Marchisio, and D.C. Altieri. 1999. Pleiotropic cell-division defects and apoptosis induced by interference with survivin function. *Nat Cell Biol.* 1:461-6.
- Li, Q., D. Hansen, A. Killilea, H.C. Joshi, R.E. Palazzo, and R. Balczon. 2001. Kendrin/pericentrin-B, a centrosome protein with homology to pericentrin that complexes with PCM-1. *J Cell Sci.* 114:797-809.
- Low, S.H., X. Li, M. Miura, N. Kudo, B. Quinones, and T. Weimbs. 2003. Syntaxin 2 and endobrevin are required for the terminal step of cytokinesis in mammalian cells. *Dev Cell.* 4:753-9.
- Lupas, A., VanDyke, M., and Stock, J. 1991. Predicting coiled-coils from protein sequences. *Science.* 252:1162-1164.
- Mackay, A.M., A.M. Ainsztein, D.M. Eckley, and W.C. Earnshaw. 1998. A dominant mutant of inner centromere protein (INCENP), a chromosomal protein, disrupts prometaphase congression and cytokinesis. *J Cell Biol.* 140:991-1002.
- Manabe, R., L. Whitmore, J.M. Weiss, and A.R. Horwitz. 2002. Identification of a Novel Microtubule-Associated Protein that Regulates Microtubule Organization and Cytokinesis by Using a GFP-Screening Strategy. *Curr Biol.* 12:1946-51.
- Martinez-Compos, M., R. Basto, J. Baker, M. Dernan, and J.W. Raff. 2004. The *Drosophila* pericentrin-like protein is essential for cilia/flagella function but appears to be dispensible for mitosis. *J Cell Biol.* in press.

- Matuliene, J., and R. Kuriyama. 2002. Kinesin-like protein CHO1 is required for the formation of midbody matrix and the completion of cytokinesis in mammalian cells. *Mol Biol Cell*. 13:1832-45.
- McGrath, J., S. Somlo, S. Makova, X. Tian, and M. Brueckner. 2003. Two populations of node monocilia initiate left-right asymmetry in the mouse. *Cell*. 114:61-73.
- McKean, P.G., A. Baines, S. Vaughan, and K. Gull. 2003. gamma-Tubulin Functions in the Nucleation of a Discrete Subset of Microtubules in the Eukaryotic Flagellum. *Curr Biol*. 13:598-602.
- Meraldi, P., R. Honda, and E.A. Nigg. 2002. Aurora-A overexpression reveals tetraploidization as a major route to centrosome amplification in p53^{-/-} cells. *Embo J*. 21:483-92.
- Mochizuki, T., G. Wu, T. Hayashi, S.L. Xenophontos, B. Veldhuisen, J.J. Saris, D.M. Reynolds, Y. Cai, P.A. Gabow, A. Pierides, W.J. Kimberling, M.H. Breuning, C.C. Deltas, D.J. Peters, and S. Somlo. 1996. PKD2, a gene for polycystic kidney disease that encodes an integral membrane protein. *Science*. 272:1339-42.
- Mogensen, M.M., J.B. Mackie, S.J. Doxsey, T. Stearns, and J.B. Tucker. 1997. Centrosomal deployment of gamma-tubulin and pericentrin: Evidence for a microtubule-nucleating domain and a minus-end docking domain in certain mouse epithelial cells. *Cell Motil. Cytoskel*. 36:276-290.
- Mogensen, M.M., A. Malik, M. Piel, V. Bouckson-Castaing, and M. Bornens. 2000. Microtubule minus-end anchorage at centrosomal and non-centrosomal sites: the role of ninein. *J Cell Sci*. 113:3013-23.
- Mollinari, C., J.P. Kleman, W. Jiang, G. Schoehn, T. Hunter, and R.L. Margolis. 2002. PRC1 is a microtubule binding and bundling protein essential to maintain the mitotic spindle midzone. *J Cell Biol*. 157:1175-86.
- Morales, C.P., S.E. Holt, M. Ouellette, K.J. Kaur, Y. Yan, K.S. Wilson, M.A. White, W.E. Wright, and J.W. Shay. 1999. Absence of cancer-associated changes in human fibroblasts immortalized with telomerase. *Nat Genet*. 21:115-8.
- Moritz, M., M.B. Braunfeld, J.W. Sedat, B. Alberts, and D.A. Agard. 1995a. Microtubule nucleation by gamma-tubulin-containing rings in the centrosome. *Nature*. 378:638-640.
- Moyer, J.H., M.J. Lee-Tischler, H.Y. Kwon, J.J. Schrick, E.D. Avner, W.E. Sweeney, V.L. Godfrey, N.L. Cacheiro, J.E. Wilkinson, and R.P. Woychik. 1994. Candidate

gene associated with a mutation causing recessive polycystic kidney disease in mice. *Science*. 264:1329-33.

- Murcia, N.S., W.G. Richards, B.K. Yoder, M.L. Mucenski, J.R. Dunlap, and R.P. Woychik. 2000. The Oak Ridge Polycystic Kidney (orpk) disease gene is required for left-right axis determination. *Development*. 127:2347-55.
- Muresan, V., H.C. Joshi, and J.C. Besharse. 1993. Gamma-tubulin in differentiated cell types: localization in the vicinity of basal bodies in retinal photoreceptors and ciliated epithelia. *J Cell Sci*. 104 (Pt 4):1229-37.
- Murphy, S.M., L. Urbani, and T. Stearns. 1998. The mammalian gamma-tubulin complex contains homologues of the yeast spindle pole body components spc97p and spc98p. *J Cell Biol*. 141:663-74.
- Nauli, S.M., F.J. Alenghat, Y. Luo, E. Williams, P. Vassilev, X. Li, A.E. Elia, W. Lu, E.M. Brown, S.J. Quinn, D.E. Ingber, and J. Zhou. 2003. Polycystins 1 and 2 mediate mechanosensation in the primary cilium of kidney cells. *Nat Genet*. 33:129-37.
- Nguyen, T., D.B. Vinh, D.K. Crawford, and T.N. Davis. 1998. A genetic analysis of interactions with Spc110p reveals distinct functions of Spc97p and Spc98p, components of the yeast gamma-tubulin complex. *Mol Biol Cell*. 9:2201-16.
- Nislow, C., C. Sellitto, R. Kuriyama, and J.R. McIntosh. 1990. A monoclonal antibody to a mitotic microtubule-associated protein blocks mitotic progression. *J Cell Biol*. 111:511-22.
- Pazour, G.J., S.A. Baker, J.A. Deane, D.G. Cole, B.L. Dickert, J.L. Rosenbaum, G.B. Witman, and J.C. Besharse. 2002a. The intraflagellar transport protein, IFT88, is essential for vertebrate photoreceptor assembly and maintenance. *J Cell Biol*. 157:103-13.
- Pazour, G.J., B.L. Dickert, Y. Vucica, E.S. Seeley, J.L. Rosenbaum, G.B. Witman, and D.G. Cole. 2000. Chlamydomonas IFT88 and its mouse homologue, polycystic kidney disease gene tg737, are required for assembly of cilia and flagella. *J Cell Biol*. 151:709-18.
- Pazour, G.J., B.L. Dickert, and G.B. Witman. 1999. The DHC1b (DHC2) isoform of cytoplasmic dynein is required for flagellar assembly. *J Cell Biol*. 144:473-81.
- Pazour, G.J., and J.L. Rosenbaum. 2002. Intraflagellar transport and cilia-dependent diseases. *Trends Cell Biol*. 12:551-5.

- Pazour, G.J., J.T. San Agustin, J.A. Follit, J.L. Rosenbaum, and G.B. Witman. 2002b. Polycystin-2 localizes to kidney cilia and the ciliary level is elevated in orpk mice with polycystic kidney disease. *Curr Biol.* 12:R378-80.
- Pazour, G.J., C.G. Wilkerson, and G.B. Witman. 1998. A dynein light chain is essential for the retrograde particle movement of intraflagellar transport (IFT). *J Cell Biol.* 141:979-92.
- Pazour, G.J., and G.B. Witman. 2003. The vertebrate primary cilium is a sensory organelle. *Curr Opin Cell Biol.* 15:105-10.
- Pereira, G., T. Hofken, J. Grindlay, C. Manson, and E. Schiebel. 2000. The Bub2p spindle checkpoint links nuclear migration with mitotic exit. *Mol Cell.* 6:1-10.
- Pereira, G., and E. Schiebel. 2001. The role of the yeast spindle pole body and the mammalian centrosome in regulating late mitotic events. *Curr Opin Cell Biol.* 13:762-9.
- Perkins, L.A., E.M. Hedgecock, J.N. Thomson, and J.G. Culotti. 1986. Mutant sensory cilia in the nematode *Caenorhabditis elegans*. *Dev Biol.* 117:456-87.
- Piel, M., J. Nordberg, U. Euteneuer, and M. Bornens. 2001. Centrosome-dependent exit of cytokinesis in animal cells. *Science.* 291:1550-3.
- Pihan, G.A., A. Purohit, J. Wallace, R. Malhotra, L. Liotta, and S.J. Doxsey. 2001. Centrosome defects can account for cellular and genetic changes that characterize prostate cancer progression. *Cancer Res.* 61:2212-9.
- Piperno, G., E. Siuda, S. Henderson, M. Segil, H. Vaananen, and M. Sassaroli. 1998. Distinct mutants of retrograde intraflagellar transport (IFT) share similar morphological and molecular defects. *J Cell Biol.* 143:1591-601.
- Porter, M.E., R. Bower, J.A. Knott, P. Byrd, and W. Dentler. 1999. Cytoplasmic dynein heavy chain 1b is required for flagellar assembly in *Chlamydomonas*. *Mol Biol Cell.* 10:693-712.
- Praetorius, H.A., and K.R. Spring. 2001. Bending the MDCK cell primary cilium increases intracellular calcium. *J Membr Biol.* 184:71-9.
- Purohit, A., S.H. Tynan, R. Vallee, and S.J. Doxsey. 1999. Direct interaction of pericentrin with cytoplasmic dynein light intermediate chain contributes to mitotic spindle organization. *J. Cell Biol.* 147:481-491.

- Quintyne, N.J., and T.A. Schroer. 2002. Distinct cell cycle-dependent roles for dynactin and dynein at centrosomes. *J Cell Biol.* 159:245-54.
- Rappaport, R. 1986. Establishment of the mechanism of cytokinesis in animal cells. *Int Rev Cytol.* 105:245-81.
- Rieder, C.L., S. Faruki, and A. Khodjakov. 2001. The centrosome in vertebrates: more than a microtubule-organizing center. *Trends Cell Biol.* 11:413-9.
- Rieder, C.L., C.G. Jensen, and L.C. Jensen. 1979. The resorption of primary cilia during mitosis in a vertebrate (PtK1) cell line. *J Ultrastruct Res.* 68:173-85.
- Rogers, K.K., P.D. Wilson, R.W. Snyder, X. Zhang, W. Guo, C.R. Burrow, and J.H. Lipschutz. 2004. The exocyst localizes to the primary cilium in MDCK cells. *Biochem Biophys Res Commun.* 319:138-43.
- Romano, A., A. Guse, I. Krascenicova, H. Schnabel, R. Schnabel, and M. Glotzer. 2003. CSC-1: a subunit of the Aurora B kinase complex that binds to the survivin-like protein BIR-1 and the incenp-like protein ICP-1. *J Cell Biol.* 161:229-36.
- Rosenbaum, J. 2002. Intraflagellar transport. *Curr Biol.* 12:R125.
- Rosenbaum, J.L., and G.B. Witman. 2002. Intraflagellar transport. *Nat Rev Mol Cell Biol.* 3:813-25.
- Saint, R., and W.G. Somers. 2003. Animal cell division: a fellowship of the double ring? *J Cell Sci.* 116:4277-81.
- Salisbury, J.L., K.M. Suino, R. Busby, and M. Springett. 2002. Centrin-2 is required for centriole duplication in mammalian cells. *Curr Biol.* 12:1287-92.
- Salminen, A., and P.J. Novick. 1989. The Sec15 protein responds to the function of the GTP binding protein, Sec4, to control vesicular traffic in yeast. *J Cell Biol.* 109:1023-36.
- Sampath, S.C., R. Ohi, O. Leismann, A. Salic, A. Pozniakovski, and H. Funabiki. 2004. The chromosomal passenger complex is required for chromatin-induced microtubule stabilization and spindle assembly. *Cell.* 118:187-202.
- San Agustin, J.T., and G.B. Witman. 2001. Differential expression of the C(s) and Calpha1 isoforms of the catalytic subunit of cyclic 3',5'-adenosine monophosphate-dependent protein kinase testicular cells. *Biol Reprod.* 65:151-64.

- Scheffers, M.S., H. Le, P. van der Bent, W. Leonhard, F. Prins, L. Spruit, M.H. Breuning, E. de Heer, and D.J. Peters. 2002. Distinct subcellular expression of endogenous polycystin-2 in the plasma membrane and Golgi apparatus of MDCK cells. *Hum Mol Genet.* 11:59-67.
- Scholey, J.M. 2003. Intraflagellar transport. *Annu Rev Cell Dev Biol.* 19:423-43.
- Schramm, C., C. Janke, and E. Schiebel. 2001. Molecular dissection of yeast spindle pole bodies by two hybrid, in vitro binding, and co-purification. *Methods Cell Biol.* 67:71-94.
- Schweitzer, J.K., and C. D'Souza-Schorey. 2002. Localization and activation of the ARF6 GTPase during cleavage furrow ingression and cytokinesis. *J Biol Chem.* 277:27210-6.
- Schweitzer, J.K., and C. D'Souza-Schorey. 2004. Finishing the job: cytoskeletal and membrane events bring cytokinesis to an end. *Exp Cell Res.* 295:1-8.
- Seong, Y.S., K. Kamijo, J.S. Lee, E. Fernandez, R. Kuriyama, T. Miki, and K.S. Lee. 2002. A spindle checkpoint arrest and a cytokinesis failure by the dominant-negative polo-box domain of Plk1 in U-2 OS cells. *J Biol Chem.* 277:32282-93.
- Shu, H.B., Z. Li, M.J. Palacios, Q. Li, and H.C. Joshi. 1995. A transient association of gamma-tubulin at the midbody is required for the completion of cytokinesis during the mammalian cell division. *J Cell Sci.* 108:2955-62.
- Skop, A.R., D. Bergmann, W.A. Mohler, and J.G. White. 2001. Completion of cytokinesis in *C. elegans* requires a brefeldin A-sensitive membrane accumulation at the cleavage furrow apex. *Curr Biol.* 11:735-46.
- Sluder, G., and E.H. Hinchcliffe. 2000. The coordination of centrosome reproduction with nuclear events during the cell cycle. *Curr Top Dev Biol.* 49:267-89.
- Somlo, S., and B. Ehrlich. 2001. Human disease: calcium signaling in polycystic kidney disease. *Curr Biol.* 11:R356-60.
- Song, L., and W.L. Dentler. 2001. Flagellar protein dynamics in *Chlamydomonas*. *J Biol Chem.* 276:29754-63.
- Sorokin, S. 1962. Centrioles and the formation of rudimentary cilia by fibroblasts and smooth muscle cells. *J Cell Biol.* 15:363-77.
- Sorokin, S.P. 1968. Reconstructions of centriole formation and ciliogenesis in mammalian lungs. *J Cell Sci.* 3:207-30.

- Stephens, R.E. 1997. Synthesis and turnover of embryonic sea urchin ciliary proteins during selective inhibition of tubulin synthesis and assembly. *Mol Biol Cell*. 8:2187-98.
- Stephens, R.E. 2000. Preferential incorporation of tubulin into the junctional region of ciliary outer doublet microtubules: a model for treadmilling by lattice dislocation. *Cell Motil Cytoskeleton*. 47:130-40.
- Sundberg, H.A., L. Goetsch, B. Byers, and T.N. Davis. 1996. Role of calmodulin and Spc110p interaction in the proper assembly of spindle pole body components. *J Cell Biol*. 133:111-24.
- Takahashi, M., A. Yamagiwa, T. Nishimura, H. Mukai, and Y. Ono. 2002. Centrosomal proteins CG-NAP and kendrin provide microtubule nucleation sites by anchoring gamma-tubulin ring complex. *Mol Biol Cell*. 13:3235-45.
- Thompson, H.M., A.R. Skop, U. Euteneuer, B.J. Meyer, and M.A. McNiven. 2002. The Large GTPase Dynamin Associates with the Spindle Midzone and Is Required for Cytokinesis. *Curr Biol*. 12:2111-7.
- Thomson, R.B., S. Mentone, R. Kim, K. Earle, E. Delpire, S. Somlo, and P.S. Aronson. 2003. Histopathological analysis of renal cystic epithelia in the Pkd2WS25/- mouse model of ADPKD. *Am J Physiol Renal Physiol*. 285:F870-80.
- Tilney, L.G., and J.R. Gibbins. 1968. Differential effects of antimitotic agents on the stability and behavior of cytoplasmic and ciliary microtubules. *Protoplasma*. 65:167-79.
- Tynan, S.H., A. Purohit, S.J. Doxsey, and R.B. Vallee. 2000. Light intermediate chain 1 defines a functional subfraction of cytoplasmic dynein which binds to pericentrin. *J Biol Chem*. 275:32763-8.
- Vagnarelli, P., and W.C. Earnshaw. 2004. Chromosomal passengers: the four-dimensional regulation of mitotic events. *Chromosoma*.
- Vogel, J.M., T. Stearns, C.L. Rieder, and R.E. Palazzo. 1997. Centrosomes isolated from *Spistula solidissima* oocytes contain rings and an unusual stoichiometric ratio of a/b tubulin. *J. Cell Biol*. 137:193-202.
- Vorobjev, I.A., and Y.S. Chentsov. 1982. Centrioles in the cell cycle. I. Epithelial cells. *J Cell Biol*. 93:938-49.
- Walther, Z., M. Vashishtha, and J.L. Hall. 1994. The *Chlamydomonas* FLA10 gene encodes a novel kinesin-homologous protein. *J Cell Biol*. 126:175-88.

- Wang, H., X. Tang, J. Liu, S. Trautmann, D. Balasundaram, D. McCollum, and M.K. Balasubramanian. 2002a. The multiprotein exocyst complex is essential for cell separation in *Schizosaccharomyces pombe*. *Mol Biol Cell*. 13:515-29.
- Wang, S., Y. Liu, C.L. Adamson, G. Valdez, W. Guo, and S.C. Hsu. 2004. The Mammalian exocyst, a complex required for exocytosis, inhibits tubulin polymerization. *J Biol Chem*. 279:35958-66.
- Wang, W., J.X. Chen, R. Liao, Q. Deng, J.J. Zhou, S. Huang, and P. Sun. 2002b. Sequential activation of the MEK-extracellular signal-regulated kinase and MKK3/6-p38 mitogen-activated protein kinase pathways mediates oncogenic ras-induced premature senescence. *Mol Cell Biol*. 22:3389-403.
- Watnick, T.J., Y. Jin, E. Matunis, M.J. Kernan, and C. Montell. 2003. A flagellar polycystin-2 homolog required for male fertility in *Drosophila*. *Curr Biol*. 13:2179-84.
- Wolff, A., B. de Nechaud, D. Chillet, H. Mazarguil, E. Desbruyeres, S. Audebert, B. Edde, F. Gros, and P. Denoulet. 1992. Distribution of glutamylated alpha and beta-tubulin in mouse tissues using a specific monoclonal antibody, GT335. *Eur J Cell Biol*. 59:425-32.
- Yoder, B.K., X. Hou, and L.M. Guay-Woodford. 2002. The polycystic kidney disease proteins, polycystin-1, polycystin-2, polaris, and cystin, are co-localized in renal cilia. *J Am Soc Nephrol*. 13:2508-16.
- Zheng, Y., M.L. Wong, B. Alberts, and T. Mitchison. 1995. Nucleation of microtubule assembly by a gamma tubulin-containing ring complex. *Nature*. 378:578-583.
- Zimmerman, W., and S.J. Doxsey. 2000. Construction of centrosomes and spindle poles by molecular motor-driven assembly of protein particles. *Traffic*. 1:927-34.
- Zimmerman, W.C., J. Sillibourne, J. Rosa, and S.J. Doxsey. 2004. Mitosis-specific anchoring of gamma tubulin complexes by pericentrin controls spindle organization and mitotic entry. *Mol Biol Cell*. 15:3642-57.